$$\iota^{**}=7/3\psi$$

Population dynamic life history models of the birds and mammals of the world

Lars Witting

Greenland Institute of Natural Resources, Box 570, DK-3900 Nuuk, Greenland.

Abstract With life history traits determining the natural selection fitnesses of individuals and growth of populations, estimates of their variation are essential to advance evolutionary understanding and ecological management during times of global change. As life history data are incomplete or missing for most species, I combine data and natural selection theory to construct a meta natural selection model of the population dynamic life history (PDLH) variation in birds and mammals. This generates PDLH models for 11,187 species of birds and 4,936 mammals, covering 29 life history and ecological traits per species. The inter-specific variation of the meta model is used to illustrate underlying natural selection mechanisms, and to explain a diverse range of population dynamic trajectories by the inclusion of population dynamic regulation. This provides essential steps towards improved evolutionary analyses and freely accessible ready-to-use online population dynamic simulations, covering most species of birds and mammals.

Keywords: Life history, population dynamics, natural selection, bird, mammal, allometry

1 Introduction

With life history traits determining the fitness of individuals they provide a gateway to the secrets of natural selection, inspiring evolutionary studies for decades. And with the average fitness of individuals being the growth rate of a population, life history traits are equally essential for our ability to understand and manage the dynamics of natural populations. Improving our skills in both areas are more critical now than ever, as the expanding demands of the growing human population challenge our living planet with climatic change and loss of habitats and biological diversity.

To progress understanding, we may analyse data at face value. The Living Planet Index (LPI 2022) is one example, where timeseries of almost 40,000 populations measure the joint trend in the diversity of animal life on Earth. According to the LPI, vertebrates are on a global retreat with an average decline of about 70% from 1970 to 2018 across all monitored populations. Luckily, the LPI is biased by outliers, with 98.6% of vertebrates across all systems showing no mean global trend (Leung et al. 2020). This discrepancy highlights the need for detailed analyses at the species level to correctly identify the conservation implications of trends.

But identified trends can have many causes, and their population biological implications are not always as straightforward as they seem. To identify the underlying causes, it is best to analyse timeseries of abundance data through mechanistic population dynamic models. Many such studies, however, especially when analysing large datasets, use mechanistic models that do not reflect the life histories and population ecological structures of the species in question (e.g., Witteman et al. 1990; Turchin and Taylor 1992; Kendall et al. 1998; Murdoch et al. 2002; Sibly et al. 2005; Knape and de Valpine 2012). By omitting the population structure from the analysis we risk false conclusions on the role of density dependence and ecological delays (Turchin 1990; Wolda and Dennis 1993; Murdoch et al. 2002; Polansky et al. 2009).

The straightforward solution is age-structured models that reflect the life histories of species. Apart from externally imposed variation and trends, the population dynamics of a species is determined by its age-structured demography and population dynamic regulation by density-dependent competition and natural selection. While it is possible to estimate the two regulating forces from population dynamic timeseries, these data are usually insufficient for the estimation of the age-structured demography. The age-structure may instead be incorporated by Bayesian analyses with demographic traits specified by priors (e.g., Hilborn et al. 1994; Punt and Butterworth 1999; Kery and Schaub 2011; Witting 2013; Lee et al. 2015; Lanzarone et al. 2017), or by an integrated population modelling that incorporates independent data on the life history, age-structure, and abundance into a joint likelihood function (e.g., Besbeas et al. 2005, 2022; Lee et al. 2015; Frost et al. 2023).

But for many if not most species with timeseries data, the required life history data are at best incomplete—

if available at all. Hence, I combine life history data and natural selection theory to estimate age-structured population dynamic life history (PDLH) models for all species of birds and mammals with an estimate of body mass. I use the same natural selection model to construct the PDLH models of all species by the adjustment of parameters, with the overall collection of single species models forming a meta natural selection model that explains much of the inter-specific life history variation from underlying variation in a few independent traits.

1.1 Natural selection

My analysis elaborates on life history theory that was developed in the 1970s and 80s (reviewed by Charlesworth 1980; Roff 1992; Stearns 1992; Charnov 1993). Here, the fitnesses of individuals in populations were analysed in relation to trade-offs and constraints, given constant relative fitnesses with frequency-independent selection. I extend this analysis with a density-frequency-dependent feedback selection to account for the evolution of the inter-specific variation.

For this I use a natural selection theory that predicts not only the evolution of body mass across species, but also much of the associated covariance in other traits. The latter is documented primarily by empirical body mass allometries, where a trait x is given as a power function $x \propto w^{\hat{x}}$ of body mass w, with $\hat{x}$ being the allometric exponent. To obtain this level of prediction, it is necessary to use an integrated selection that incorporates the population ecological structure of population dynamic feedback. The essential feedback runs from the life history over the population dynamic growth and associated frequency-dependent selection by the density-dependent interactive competition that occurs among the individuals in a population, a selection that is described by the theory of Malthusian relativity (Witting 1997, 2008, 2017a,b). To understand the essential role of population dynamic feedbacks in natural selection, let us compare classical frequency-independent selection and Malthusian relativity.

The success of classical life history theory reflects its ability to determine whether a species has evolved by directional selection towards an evolutionary equilibrium, known also as a selection attractor. Being based on frequency-independent selection, this success may appear as somewhat of a paradox as it ignores the density-frequency-dependent interactions that occur among individuals in natural populations. These interactions are typically competitive, and as they distribute the available resources differentially across individuals, they are directly influencing the relative fitnesses among variants (see e.g. Hardy and Briffa 2013). This makes the relative fitness of a variant dependent not only on the frequencies of the other life history variants in the population, but this frequency dependence is even density-dependent as individuals encounter other individuals in competition more often at high population densities. How can a life history theory that ignores these basis rules of competition have any success with evolutionary predictions?

Population dynamic feedback selection takes the alternative game theoretical route (Maynard Smith and Price 1973; Maynard Smith 1982), where it uses asymmetrical interactions (Parker 1974) and Continuously Stable Strategies (Eshel and Motro 1981; Taylor 1989; Christiansen 1991) to analyse for life history evolution by the selection of the density-frequency-dependent interactive competition (including also energetic trade-offs that cannot evolve).

Where most game theory deal with differences in behavioural strategies of interaction, population dynamic feedback selection focusses on the competitive asymmetry of life history traits like body mass, group size, the male/female division of labour, and the associated sexual reproduction attraction of two genders. These interactive qualities are inversely related to population dynamic growth by the quality-quantity trade-off (Smith and Fretwell 1974; Stearns 1992), the costs of resource sharing, the two-fold cost of males (Maynard Smith 1971), and the two-fold cost of meiosis (Williams 1975). Their interactive selection is thus happening at the cost of population dynamic growth, and this generates a population dynamic feedback loop that selects for an energetic balance between the life history and its associated population growth, population abundance, level of interference competition, and interactive selection (Witting 1997, 2002, 2008).

Where fitness distributions in natural populations verify classical life history theory, the verification of feedback selection includes also predictions of evolution in time and of the differentiation in life histories among species and higher taxa. To verify the latter we start from the origin of replicating molecules, where natural selection selects for a gradual unfolding of population dynamic feedback selection, with this unfolding selecting lifeforms from molecular replicators over prokaryote and protozoa like self-replicating cells to multicellular animals (Witting 2017b). This prediction includes the selection of transitions in replicating units from asexual replicators over sexually reproducing pairs and cooperative breeders to fully evolved eusocial colonies (Wit-

ting 1997, 2002, 2007). Another essential prediction is the deduction of the inter-specific body mass allometries (Witting 1995, 2017a) that I use in the present paper to extrapolate life history models across birds and mammals.

The contrast between frequency-independent and density-frequency-dependent fitnesses seems to place classical life history theory and population dynamic feedback selection in direct opposition to one another. Yet—even for multicellular animals with interactive competition and a fully evolved feedback selection—it is possible to consolidate the two frameworks into a coherent whole by treating the classical method as an instant description of current selection, and population dynamic feedback selection as a description of natural selection through time, including predictions of life history variation among species. This is possible because the density-frequency-dependence is frozen at instant moments in time, where the population densities and levels of interference are given, and the distribution of variants and relative fitnesses are constant.

It is thus relatively easy to apply the mathematical framework of constant relative fitnesses to the current fitness distributions in natural populations and thereby estimate the outcome of natural selection in relation to the current physiological and ecological trade-offs of the species. Yet—as the population density, level of interference, composition of variants, and relative fitnesses change with evolution—the frequency-independent framework is usually too rigid for realistic predictions of evolutionary variation across species and time (Witting 1997, 2008).

This limit of traditional theory is among others identified by predictions that distort the inter-specific life history variation relative to observations. This is evident in allometric theory, where hypotheses of metabolic scaling are dominated by physiological explanations (e.g., Kozlowski and Weiner 1997; West et al. 1997, 1999; Banavar et al. 1999; Brown and West 2000; Makarieva et al. 2003; Glazier 2005) that extend into a metabolic theory of ecology (Brown et al. 2004) with additional life history models for the natural selection of mass (Brown and Sibly 2006). This selection is essentially frequency-independent, with Fisher's (1930) fundamental theorem of natural selection predicting an increase in average fitness during the selection of mass, as measured by an increase in the growth rate (r) and/or carrying capacity (k) of the population. Yet, the evolution of increased mass across natural species is characterised by a decline in r and k (Fenchel 1974; Damuth 1981, 1987), and this shows that evolution overall has taken a direction diametrically opposite to the direction

of physiologically explained body mass allometries.

This failure of Fisherian selection reflects—most likely—that it is a special limit case (Witting 1997, 2000a) that applies only in the absence of frequency-dependent interactive competition (as expected e.g. for replicating molecules at the origin of life). The underlying concept of a natural selection increase in average fitness vanishes with the emergence of frequency-dependent selection, and this allows for a selection decline in r and k. And by explicitly analysing the selection of density-dependent interactive competition, population dynamic feedback selection provides the first and so far only theory where the inter-specific allometric exponents of several physiological and ecological traits are explained by the natural selection of metabolism and mass (Witting 1995, 2017a), including the observed decline in r and k with a selection increase in mass. This prediction explains not only well-known Kleiber (1932) scaling with typical $\pm 1/4$ and $\pm 3/4$ exponents for terrestrial taxa that forage in two spatial dimensions predominantly, but also corresponding $\pm 1/6$ and $\pm 5/6$ exponents for pelagic species that forage in three dimensions (Witting 1995). Additional predictions explain i) allometric transitions from prokaryotes to protozoa and multicellular animals (Witting 2017a,b), ii) a curvature in the metabolic allometry of placentals (Witting 2018), and iii) allometric scaling differences in body mass trajectories of the fossil record describing biological evolution over millions and billions of years (Witting 2020).

In the present study I estimate the life history and ecological traits of the population dynamic feedback cycle. An essential component of the feedback is the interactive foraging in overlapping home ranges that generates net energy for reproduction, with reproduction driving the population dynamic growth that determines the population abundance, which in term affects the home range overlap and associated frequency of interactive competition that selects net energy into mass, as the larger-than-average individuals monopolise resources during interactive competition. This feedback selection of mass is constrained by the physiological energetics of individuals, the population dynamic growth, and the resulting foraging ecology where individual opportunities are constrained by the spatial dimensionality of habitats, the abundance of the population, and the trait values of the other individuals in the population. These ecological constraints adjust the selected allometries in relation to the spatial dimensionality of the ecological packing of home ranges (Witting 1995), generating Kleiber scaling by a mass-rescaling selection that maintains the net energy of the organism during

the selection of mass (Witting 2017a).

By estimating the essential traits of the feedback cycle, the PDLH models in the present study describe the intra-specific flow of energy as selected by population dynamic feedback selection. Yet, the estimated models focus only on the average trait values, and not on the underlying intra-population differentiation in energy and fitness that drives natural selection. For insights on the latter you may consult theoretical studies like Witting (1997, 2002, 2008, 2017a,b).

Having estimated the life history traits across birds and mammals, I use the intra- and inter-taxa variation of birds, placentals (minus bats), marsupials, and bats to illustrate how the physiology, demography, and ecology of natural species are selected in a mutual balance that follows the predictions of population dynamic feedback selection (Section 3.2). And in Section 3.3, I illustrate how the single species models are relatively easily extended into population dynamic simulations with a diverse set of timeseries explained by the inclusion of population dynamic regulation.

2 Methods

To estimate the PDLH models across species, I combined a wide range of life history and ecological data from databases and the scientific literature (see data section 2.5). I check the data of each trait for outliers and use allometric calculations to estimate missing parameters for all species with a data-based estimate of body mass (Section 2.6). The resulting PDLH models combine the four components of individual growth, demography, life history energetics, and population ecology, with the parameters of each of the four sub-models given below.

2.1 Individual growth

Individual growth with age (a) is described by

t_p: the gestation (mammals) or incubation (birds) period;

t_0: the age at birth (mammals) or hatching (birds), with $t_0 = 0$;

t_f: the age at maximum growth, i.e., inflection point;

t_j: the age at weaning (mammals) or fledging (birds);

t_d: the age at independence from parents, $t_j \leq t_d < t_m$ with t_m being the age at reproductive maturity, assuming complete parental care for $a < t_d$, and no care for $a \geq t_d$;

w: the average body mass of adults (sexual dimorphism is not considered although it is pronounced in some species);

w_x: the mass at $t_x = t_0$, t_f, t_j or t_d, with relative mass $\tilde{w}_x = w_x/w$.

Embryotic growth from age $-t_p$ to t_0 is calculated by the Gompertz (1832) growth curve following common regularities for birds and mammals (Ricklefs 2010), with the asymptote ($\tilde{w}_\infty$) of the Gompertz growth function $\tilde{w}_a = \tilde{w}_\infty e^{-be^{-ka}}$ being 2.5 times $\tilde{w}_0$ for embryotic growth, and the growth rate $k = 1.9t_p^{-0.9}$ being approximately inversely proportional to the gestation/incubation period. This implies the following embryotic growth

$$\tilde{w}_a = 2.5\tilde{w}_0 e^{\ln[0.4\tilde{w}_p/\tilde{w}_0]e^{-1.9t_p^{-0.9}(a+t_p)}} \tag{1}$$

with age $-t_p \leq a < 0$ given in days and relative mass at $-t_p$ being $\tilde{w}_p = e^{(e^{1.9t_p^{0.1}}-1)\ln 0.4 + \ln \tilde{w}_0}$.

Growth after birth/hatching is estimated by Richards (1959) growth function, with species specific data-estimates of the inflection point obtained by least-square fitting to growth data obtained from the literature [growth curve supplementary information (SI)]. This growth function

$$\tilde{w}_a = \frac{\tilde{w}_0}{[\tilde{w}_0^z + (1 - \tilde{w}_0^z)e^{-ka}]^{1/z}} \tag{2}$$

passes through $\tilde{w}_0$ at $a = t_0 = 0$ and $\tilde{w}_j$ at $a = t_j$, with $k = -\ln[\tilde{w}_0^z(\tilde{w}_j^{-z} - 1)/(1 - \tilde{w}_0^z)]/t_j$ and a relative adult mass of unity ($\tilde{w}_\infty = 1$). The inflection point $\tilde{w}_f$ is calculated given the fitted or extrapolated estimates of the shape parameter z, with $\tilde{w}_f$ increasing from zero to 0.5 when z increases from -1 to 1.

There is only little information available on the age (t_d) and weight ($\tilde{w}_d$) at independence from parents (but see e.g. Millar et al. 1986; Lloyd 1987; Johansson et al. 2021). While I treat independence as a knife-edge parameter, real independence is a gradual development. Independence is often later than weaning in mammals, and closer to fledging in birds [with median $\tilde{w}_j$ being 0.33 (cv:0.77) and 0.84 (cv:0.24) in mammals and birds for the data in the present study]. With no clear data estimate, I approximate the minimum mass at independence by median fledging mass in birds, assuming that parents invest at least 84% in the mass of offspring (either directly, or indirectly by protecting the foraging area of offspring). The relative mass at independence is thus $\tilde{w}_d = \max(\tilde{w}_j, 0.84)$, with t_d being the solution to eqn 2 at $\tilde{w}_d$.

2.2 Demography

The demographic traits include

p_{ad}: the annual survival probability of adults as available in the scientific literature (geometric mean across adult age-classes when possible);

q_{ad}: the annual mortality of adults, $q_{ad} = 1 - p_{ad}$;

t_m: female age at reproductive maturity, $t_m = t_s + t_p$ with t_s being sexual maturity;

t_r: the expected reproductive period of females that survive to t_m, as $t_r = \min[4/mp_{ad}^{t_m}, 1/(1 - p_{ad})]$ from Appendix A;

t_g: generation time as the average age of reproduction, as $t_g = t_m + t_r - 1$ from Appendix A;

t_l: the maximum lifespan of an individual;

l_m: the probability that a new-born survives to t_m, estimated as $l_m = 2/R$ by eqn 3;

m: the average number of offspring/eggs produced per female per year, i.e., $m = m_b\, m_f$ where m_b is the average brood/clutch size and m_f the average brood frequency; and

R: expected lifetime reproduction as the average number of offspring produced over the expected reproductive period for females that survive to t_m, estimated as $R = t_r m$.

These parameters are estimated for species that are assumed to be naturally selected around a population dynamic equilibrium with a per-generation growth rate of unity

$$\lambda = l_m t_r m/2 = 1, \tag{3}$$

assuming an even sex ratio and a pairwise reproducing unit. While many birds and mammals have more elaborate reproducing units, I do not attempt to estimate e.g. the frequencies of, and number of helpers in, co-operative breeding units across birds and mammals (the models of these species should be interpretated accordingly).

2.3 Life history energetics

The demographic traits are linked to the energetics of the organism by

w_ϵ: body mass as combustion energy (SI unit J); obtained as $w_\epsilon = c_{w \to d} c_{d \to \epsilon} w$, with w being mass in grams, $c_{w \to d}$ the conversion of wet organic matter to dry [0.40 for birds (Mahoney and Jehl 1984), and 0.35 for mammals (Prothero 2015)], and $c_{d \to \epsilon}$ the conversion of dry matter to energy [22.6 kJ/g from Odum et al. (1965) and Griffiths (1977)];

$\underline{\beta}$: basal mass-specific metabolism (SI unit W/g);

β: field mass-specific metabolism (SI unit W/g) also the pace (SI unit Hz for w as w_ϵ) of the metabolic work carried out per unit body mass;

α: the handling of net resource assimilation (resource handling in short, SI unit J), defined as net energy (ϵ) generated per metabolic pace, with $\alpha = \epsilon/\beta$;

ϵ: the net assimilated energy of adults is the product ($\epsilon = \alpha\beta$; SI unit W) of resource handling (α) and metabolic pace (β). Following the selection attractor of sexually reproducing pairs (Witting 2002), half of the joint net energy (2ϵ) of the female/male unit is allocated to reproduction, while the other half is used in intra-specific interactions. Net energy is estimated as $\epsilon = w_e \acute{\beta} R/t_r$ from eqn 4; and

ϵ_g: average gross energy $\epsilon_g = w\beta + \epsilon/2$ (SI unit W; given as a relative measure $\tilde{\epsilon}_g = \epsilon_g/\epsilon$) is total field metabolism plus net energy allocated to reproduction. The latter is $\epsilon/2$ as the reproducing unit uses half of their net energy in reproduction, with the metabolism of intra-specific interactions burning the other half.

Net energy defines lifetime reproduction by the number of offspring it produces. Assuming complete parental investment until t_d, we have

$$R = \epsilon t_r/\acute{\beta} w_\epsilon \tag{4}$$

where

$$\acute{\beta} = (w_d + t_e \beta \bar{w}_d)/w \tag{5}$$

is a scaling parameter that scales w_ϵ to the mass at independence (w_d) and accounts for energy that is metabolised by the offspring during parental care ($t_e = t_p + t_d$), with $t_e \beta \bar{w}_d$ being the energy that is metabolised by the offspring during t_e, assuming constant mass-specific metabolism (β) and an average size

$$\bar{w}_d = \frac{1}{t_e} \int_{a=-t_p}^{t_d} w_a\, da \tag{6}$$

that is calculated by the growth model of eqns 1 and 2, with $-t_p$ being the negative age at fertilisation.

2.4 Population ecology

Important population ecological components include

N: population density (abundance), as the number of animals per km^2;

b: the standing biomass of the population, as $b = wN$ in kg/km^2;

ϵ_n: the energy consumed by the population, calculated as $\epsilon_n = \epsilon_g N$ (in W/km^2);

h: the average home range of an individual (in km^2);

h_o: the average home ranges overlap $h_o = hn$, given as home range divided by the available of space ($1/N$) per individual;

v: the frequency of competitive encounters per individual per unit home range overlap, given as a relative measure $v \propto v_f/l_f$, where $l_f \propto h^{1/d}$ is the length of foraging tracks (proportional to the dth root of the home range in d-dimensions) and $v_f \propto \beta_\beta w^{1/2d}$ the average foraging speed obtained from allometric correlations where β_β is the intercept of the metabolic allometry $\beta = \beta_\beta w^{-1/2d}$ (Witting 1995, 2017a); and

I: intra-specific interference competition per individual, calculated as a relative measure $I \propto h_o v \propto Nhv$ from the overlap in home ranges and the frequency of encountering other individuals per unit home range overlap (Witting 1995, 2017a). These I estimates are rescaled for a log value ($\iota = \ln I$) of unity at the median across all species of birds.

2.5 Data

My study extends on the data used by Witting (2023a), with all literature estimates treated as raw data. A trait of a species that is calculated from the raw data of that species is included in my definition of data.

I use the BirdLife (2022) taxonomy for birds, and MDD (2023) taxonomy for mammals, with some subspecies with separate body mass estimates categorised as species. Body mass data were obtained from several sources including Smith et al. (2004), Dunning (2007), Jones et al. (2009), Weisbecker et al. (2013), Myhrvold et al. (2015), Tobias et al. (2021), and Herberstein et al. (2022). Demographic parameters on reproduction, time periods, and growth were achieved from many datasets including Jetz et al. (2008), De Magalhães and Costa (2009), Jones et al. (2009), Myhrvold et al. (2015), and

del Hoyo et al. (1992–2011), with growth curve data and survival rates obtained from an independent literature search, including survival estimates from McCarthy et al. (2008), DeSante and Kaschube (2009), Ricklefs et al. (2011), del Hoyo et al. (1992–2011), Wilson and Mittermeier (2009–2014), and Beauchamp (2023). Ecological parameters included population densities from Damuth (1987) and Santini et al. (2018), and home range areas from Tucker et al. (2014), Tamburello et al. (2015), and Nasrinpour et al. (2017) with an independent literature search for marine mammals and bats. Basal metabolic rates were obtained primarily from McNab (2008) for mammals and from McKechnie and Wolf (2004) for birds, with field metabolism for both taxa from Hudson et al. (2013).

Altogether, I obtained 113,511 trait values from 612 literature sources. Some of these data are the same, and I put more weight on commonly agreed estimates by using the average trait values of the available raw data for each trait per species. This resulted in 63,385 species specific raw data, with Table 1 listing the number of species with raw data for different traits.

These data are distributed relatively evenly across the taxonomic groups considered. For each body mass estimate, I had on average data for 2 additional traits per bird species and 4 additional traits per mammal, including 4.7, 5.4, and 2.5 additional traits per placental, marsupial, and bat. For the traits in Table 1, I had 21% raw data for birds and 24% for mammals, with 26% for placentals, 31% for marsupials, and 16% for bats. In other words, I had 79% and 76% missing parameters to estimate for birds and mammals.

All data were checked for outliers (except body mass; see outlier SI), with a total of 346 outliers removed. I list the literature references of all accepted data (follow the letter codes in the SI on estimates and SI on data references), and for the underlying data of derived traits calculated from one or two underlying traits with data. Higher-level data calculated from three or more traits are treated as data but with no specific reference.

2.6 Estimating missing values

Missing values were estimated by inter-specific body mass allometries, invariances, and traits combinations following the allometric model of Witting (2017a) and the estimation sequence in Appendix B. Five filters (see filter SI) were used to improve t_r estimation and capture unrealistic values like *i*) small lifespan estimates due to under-sampling, *ii*) low survival rates due to e.g. confounding issues with migration, *iii*) small estimates of gross energy due to estimation uncertainty,

	w	$\tilde{w}_0$	$\tilde{w}_j$	$\tilde{w}_f$	β	$\underline{\beta}$	t_p	t_j	t_s	t_m	t_l	m_b	m_f	p_{ad}	N	h
Ave.	11187	774	207	155	76	470	2237	1819	1210	681	1667	7157	6986	998	1438	249
Mam.	4936	1868	1059	101	57	713	2217	2040	1999	935	2614	3511	2148	310	1110	456

	w	β	t_x	m	R	l_m	ϵ	α	N	b	ϵ_n	h	h_o	I
Exp.	1	$-\frac{1}{2d}$	$\frac{1}{2d}$	$-\frac{1}{2d}$	0	0	$\frac{2d-1}{2d}$	1	$\frac{1-2d}{2d}$	$\frac{1}{2d}$	0	1	$\frac{1}{2d}$	0

Table 1: Top table: The number of birds (Ave) and mammals (Mam) with data for different traits. Bottom table: The theoretical exponents of inter-specific allometries, as predicted by population dynamic feedback selection; see mathematical deduction in Witting (1995, 2017a) or graphical deduction in Witting (2023a) [$t_x \in \{t_p, t_j, t_s, t_m, t_r, t_g, t_l\}$]. The theoretical exponents dominate the missing value estimators that are based on few data, while data-based exponents take over in estimators with several data (see Section 2.6 for details). The theoretical exponents depend on the spatial dimensionality (d) of the ecological packing of home ranges (see Table 2).

Class	Order	Family	d
Aves	-	-	2
Mammalia	-	-	2
Mammalia	Primates	-	3
Mammalia	Carnivora	-	2
Mammalia	Carnivora	Otariidae	3
Mammalia	Carnivora	Odobenidae	3
Mammalia	Carnivora	Phocidae	3
Mammalia	Cetacea	-	3

Table 2: The dimensionality (d) of the ecological packing of home ranges follows the classification in Witting (2017a).

and *iv*) unrealistic parameter combinations on individual growth.

Allometric estimators: Missing values of the mass-dependent parameters in Table 1 were calculated as allometric functions of mass and, dependent upon the availability of data for species closely related to the missing-parameter-species, these calculations were performed by estimators at the genus, family, order, or class taxonomic level. Mass-specific metabolism, e.g., was calculated as

$$\beta(l, n) = \beta_\circ w^{\hat{\beta}} \qquad (7)$$

with l denoting the taxonomic level of the estimator, and n the number of $\{w, \beta\}$ data points at that level. The allometric exponent ($\hat{\beta}$) and intercept ($\beta_\circ$) were estimated as joint functions

$$\begin{aligned} \hat{\beta} &= q\,\hat{\beta}_d + (1-q)\,(\hat{\beta}_e + q_e) \qquad (8) \\ \beta_\circ &= q\,\beta_{\circ,d} + (1-q)\,\beta_{\circ,e} \end{aligned}$$

of the theoretical expectation [subscript e; from Witting (1995, 2017a) with $\hat{\beta}_e = -1/2d$ from Table 1 and d

from Table 2, with $\beta_{\circ,e}$ being the geometric mean of the intercepts of the n species with data given the expected exponent $\hat{\beta}_e$] and the data of the estimator [subscript d; with $\hat{\beta}_d$ and $\beta_{\circ,d}$ being point estimates from linear regression on double logarithmic scale, with $\hat{\beta}_d$ being truncated at a minimum ($\hat{\beta}_d \geq \hat{\beta}_e - q_d$) and maximum ($\hat{\beta}_d \leq \hat{\beta}_e + q_d$) allowed distance q_d from the expectation $\hat{\beta}_e$]. The weight

$$\begin{aligned} q &= 0 & \text{for } n < 3 \qquad (9) \\ q &= e^{-e^{-q_g(n-q_n)}} & \text{for } n \geq 3 \end{aligned}$$

of the data increased monotonically from zero to one as a function of n, with $q_g > 0$ and $q_n > 0$ being tuning parameters. Having no clear theoretical expectation of the exponents for $\tilde{w}_0$, $\tilde{w}_j$, m_b, and m_f their theoretical values were replaced with exponents from linear regressions across all raw data for birds, placentals (minus bats), marsupials, and bats (BPMB). Invariance estimators were used for lifetime reproduction (R) and the inflection parameter z. Invariances were estimated as the average of the data at the taxonomic level of the estimator.

Given the taxonomies and available data, I allowed for the construction of up to 4218 different estimators for each trait covering the four taxonomic levels, with 2676, 1168, 119, and 257 potential estimators for BPMB (placentals, marsupials, and bats have the same class estimator). The estimators of each trait were grouped in a 4x4-matrix that covers the four taxonomic levels from genus to class and the four BPMB groups. The four tuning parameters q_g, q_n, q_e, and q_d were estimated separately for each matrix entry. This was done by a numerical minimization of the sum of squares of the difference between the data of the relevant estimators and the estimator predicted values of those data given the data of the other species of those estimators.
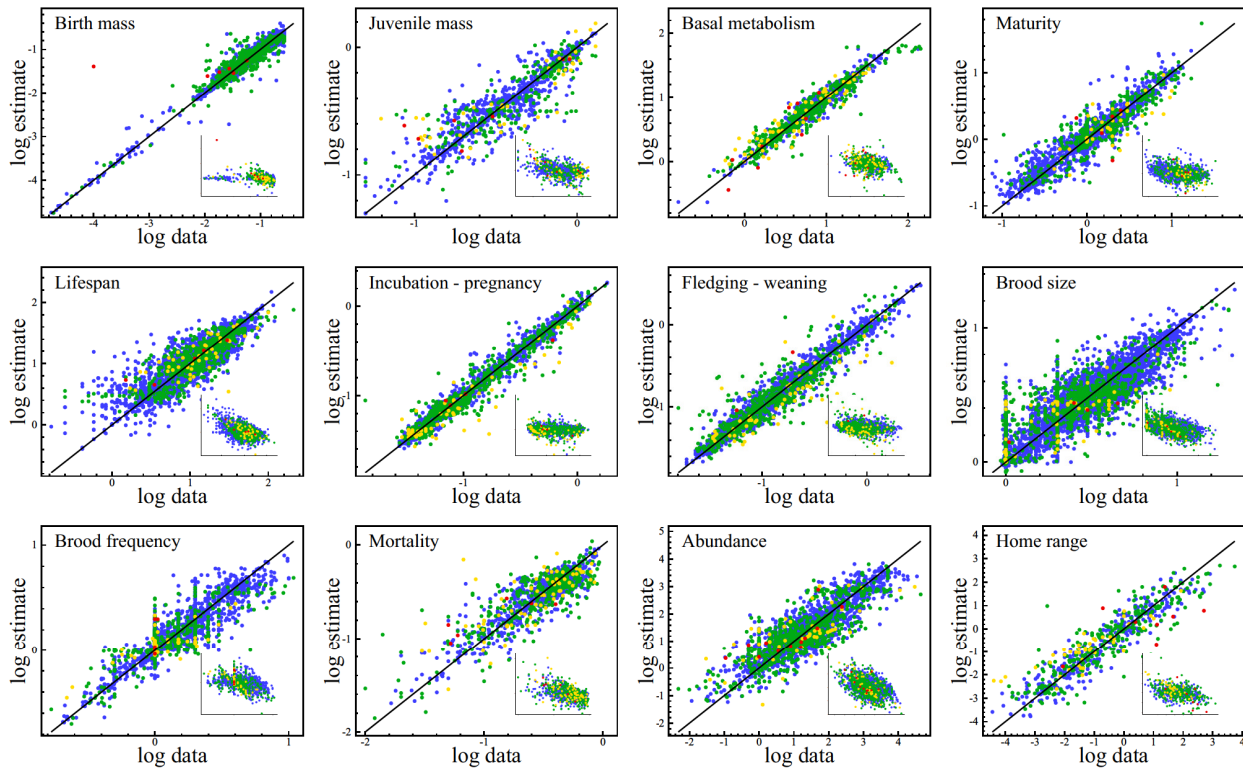
Figure 1: Cross-validation plots. The estimation of missing parameters by allometric correlations was cross-validation optimised to provide the best predictions of the available data (see Section 2.6 for details). The 15 plots illustrate the relationships between the data and their best cross-validation estimates on double logarithmic scale. Residuals are shown in insert plots, and the average precisions of the estimates are given in Table 3. Estimator levels: genus (blue), family (green), order (yellow), and class (red); with points of the latter sitting on top of the former.

With the estimated medians of q_n and q_g of eqn 9 being 3 and 2.1 respectively, most sets of estimators had a step q transition from zero to one for estimators with more than three data points. Yet, with an estimated maximum value of 18 for q_n and an estimated minimum value of 0.1 for q_g, some estimators had a slower transition, with $q = 1$ data-based estimation requiring more data. The q_e adjustment in eqn 8 of the theoretical exponent was generally low, with a median value around zero. Yet, with a standard deviation (sd) of 0.091 and minimum/maximum values of ± 0.2, optimal estimation requires adjustment in some cases (I did not allow for larger q_e adjustments than ± 0.2).

With the median truncation distance (q_d) for the data estimated exponents being 0.17, the estimators were generally allowing for some variation around the expectation, yet truncating large deviations that did not improve estimation precision. The optimal level of this truncation varied from 0.05 to 0.65, with a sd of 0.16.

Estimation level: Missing values were estimated at different taxonomic levels dependent upon the available data. The precision of an allometric estimate will generally increase with the number of data and—due to the phylogenetic dependence of closely related species—precision will generally decline with taxonomic level from genus over family and order to class. With the number of data points for any trait increasing with taxonomic level, we expect a trade-off where an estimator based on few data at a low taxonomic level will, at some point, provide a better estimate than an estimator with many data at a higher taxonomic level.

To determine the data limits—where lower-level estimators are preferred over higher-level estimators with more data—I constructed a hierarchical estimator that used the lowest taxonomic level with a given number (n_d) of data points. The optimum of this number was estimated by a numerical cross-validation that minimized the sum of squares of the difference between raw data and their predicted values, with the predicted data

	$\tilde{w}_0$	$\tilde{w}_j$	β	$\underline{\beta}$	t_m	t_l	t_p	t_j	m_b	m_f	p_{ad}	q_{ad}	N	h	Avg.
Genus	0.10	0.11	0.13	0.13	0.14	0.18	0.05	0.08	0.04	0	0.12	0.21	0.92	0.88	0.10
Family	0.25	0.26	0.25	0.24	0.25	0.43	0.12	0.20	0.18	0.04	0.20	0.33	1.30	1.26	0.26
Order	0.42	0.35	0.33	0.31	0.40	0.51	0.21	0.33	0.35	0.21	0.23	0.42	1.47	1.54	0.41
Class	0.93	0.45	0.47	0.41	0.65	0.67	0.45	0.57	0.53	0.28	0.29	0.53	1.66	2.15	0.60
Birds	0.14	0.11	0.22	0.21	0.16	0.30	0.08	0.13	0.13	0.01	0.18	0.30	1.25	1.19	0.18
Placentals	0.28	0.25	0.27	0.26	0.33	0.37	0.14	0.25	0.20	0.24	0.24	0.47	1.24	1.34	0.33
Marsupials	0.38	0.37	0.15	0.15	0.31	0.51	0.20	0.22	0.19	0.20	0.21	0.24	1.12	1.20	0.30
Bats	0.33	0.21	0.26	0.24	0.33	0.55	0.25	0.30	0.09	0.12	0.27	0.35	1.85	1.06	0.32
Avg.	0.32	0.26	0.27	0.25	0.31	0.40	0.15	0.24	0.19	0.03	0.20	0.35	1.31	1.39	0.28

Table 3: Estimation uncertainty. The geometric means of the standard deviations of the log of the cross-validation data/estimate ratios across allometric estimators, illustrating estimation uncertainty across traits, estimation levels, and major taxonomic groups (excluding class level estimators for the latter). See Section 2.6.

values of a species being predicted from the raw data of the other species.

Given the optimal missing value estimation of eqns 7 to 9, the minimization of the sum of squares between the raw data and their predicted values determined that the more precise estimates of missing values were obtained with a n_d parameter around unity. Taxonomic proximity was thus prioritized over sample size due to phylogenetically correlated traits, with missing values being calculated at the lowest taxonomic level with one or more raw data of the required parameters. Genus (g) was prioritized over family (f), family over order(o), and order over class (c).

Estimation uncertainty: The cross-validation in Fig. 1 illustrates how well the data are predicted by the lowest taxonomic level estimators (that exclude the estimated data points). There is a close to linear relation for all traits, except that some traits tend to be overestimated for smaller masses (see e.g. residual plots for lifespan and abundance).

To describe the uncertainty of each missing parameter estimate, I used the cross-validation of the relevant estimator to calculate the sd of the natural logarithm of the data/estimate ratio across all the data of that estimator (this coefficient of variation like measure is listed for all parameter estimates from estimators with two or more data points).

For all traits with allometric estimators, Table 3 lists the geometric mean of the sd of the log ratios across all estimators at the four taxonomic levels, and all estimators for birds, placentals, marsupials, and bats. Exclud-

ing the estimators for abundance (N) and home range (h) where the average sd is 1.31 and 1.39, the precisions are generally acceptable. For the remaining traits, the geometric mean of the sd of the log ratio range from 0.03 for brood frequency to 0.40 for lifespan, with the overall average across all traits being 0.28. The precision is generally declining with the taxonomic level of the estimator, with the average sd being 0.10 at the genus level, 0.26 at the family level, 0.41 at the order level, and 0.60 at the class level. With an average sd of 0.18 birds have the best estimation precision, followed by marsupials (0.30), bats (0.32), and placentals (0.33).

3 Results

3.1 Estimates

The proportions of the different estimation levels across all species are shown in Fig. 2 for a subset of parameters. Mammals have a larger fraction of data than birds for most traits, yet even for birds 99%, 93%, 92%, 88%, 74%, and 87% of the estimates for m, N (and b), t_p, t_j, t_m and t_l are at or below the family level. The corresponding values are 100%, 86%, 99%, 99%, 98%, and 97% for mammals, where 46%, 22%, 45%, 41%, 37%, and 47% of the estimates are data.

For mass-specific metabolism 5% and 15% of the estimates for birds and mammals are data, and 84% and 95% of the estimates are at or below the family level. For survival, 8% and 4% of the estimates for birds and mammals are data, and 88% and 75% are at or below the family level. The mass at birth ($\tilde{w}_0$) and weaning ($\tilde{w}_j$) have a strong data base in mammals (37% & 21%
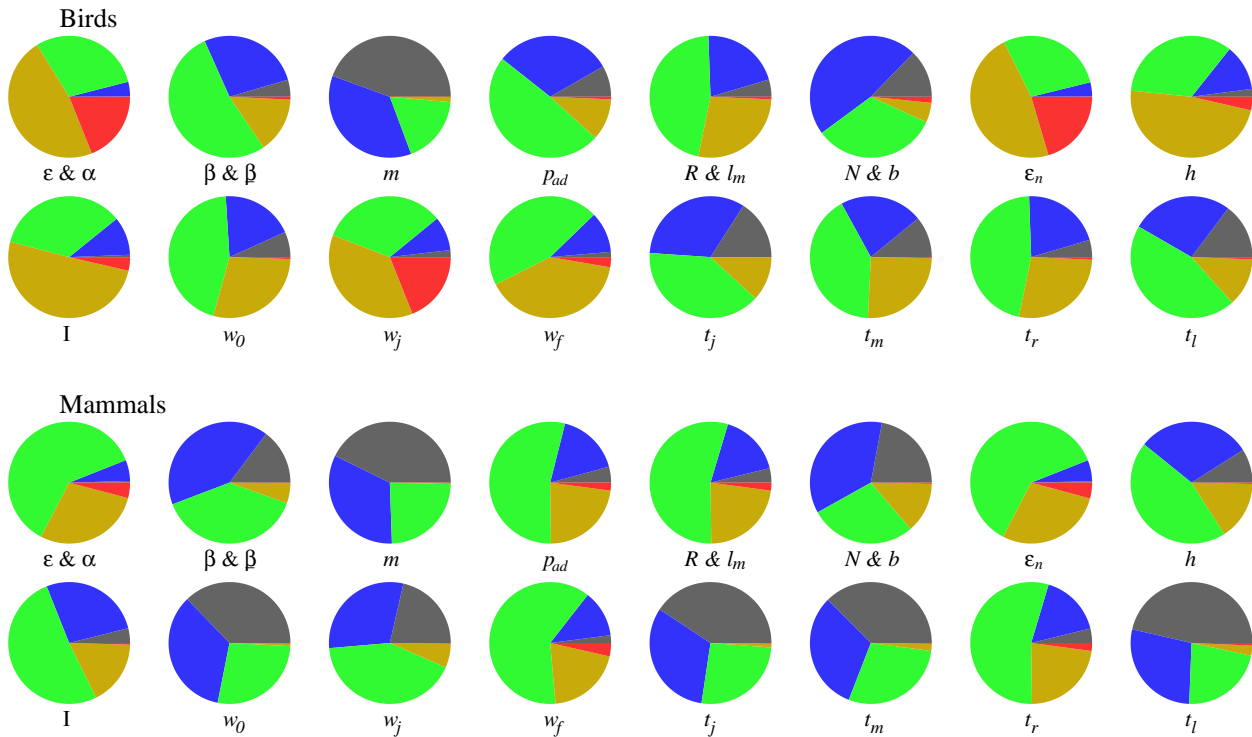
Figure 2: Estimator distributions for different traits. The proportions of estimates at the data (black), genus (blue), family (green), order (yellow), and class (red) levels for 11,187 species of birds and 4,936 species of mammals.

are data), but less so in birds especially for mass at fledging (7% & 2% are data).

Traits that are less supported by data are typically calculated from at least two independent parameters, with estimator levels listed by the parameter that is estimated at the highest taxonomic level. These traits include ϵ, α, R, l_m, ϵ_n, I, t_r, and t_g. Yet, even net energy (ϵ) and resource handling (α)—which are calculated from seven underlying parameters—have 34% and 68% of the estimates in birds and mammals at or below the family level.

The estimated life history variation is plotted as allometric functions of body mass for birds and placentals in Fig. 3 and marsupials and bats in Fig. 4. These plots illustrate that most of the estimates are contained within the overall parameter space of the data.

Table 4 list the growth and demographic parameters, and Table 5 the energetic and population ecological parameters, for 20 randomly chosen species. The complete set with 11,187 models for birds, and 4,936 models for mammals, are listed in the model SI. These estimates illustrate a wide diversity of traits, with Table 6 summarising the median values of selected traits for birds, placentals (minus bats), marsupials, and bats (BPMB). Table 6 includes also estimates of allometric intercepts presenting the expected traits at the mean of the median masses of birds and mammals (58g), and the 95% ranges of the inter-specific variation in the four taxa.

3.2 Life history evolution

In this section I use the estimated models to illustrate how population dynamic feedback selection reconciles large parts of the inter-specific life history covariance of the four BPMB taxa.

Metabolism, net energy, & body mass: The evolution of metabolism, net energy, and body mass is tightly linked to one another by population dynamic feedback selection. To examine this let us start from the selected inter-specific range in body mass, which covers 4.8, 7.9, 4, and 2.7 orders of magnitude for BPMB. The median marsupial is 127% larger than the median placental that is 317% larger than the median bird that is 157% larger than the median bat.
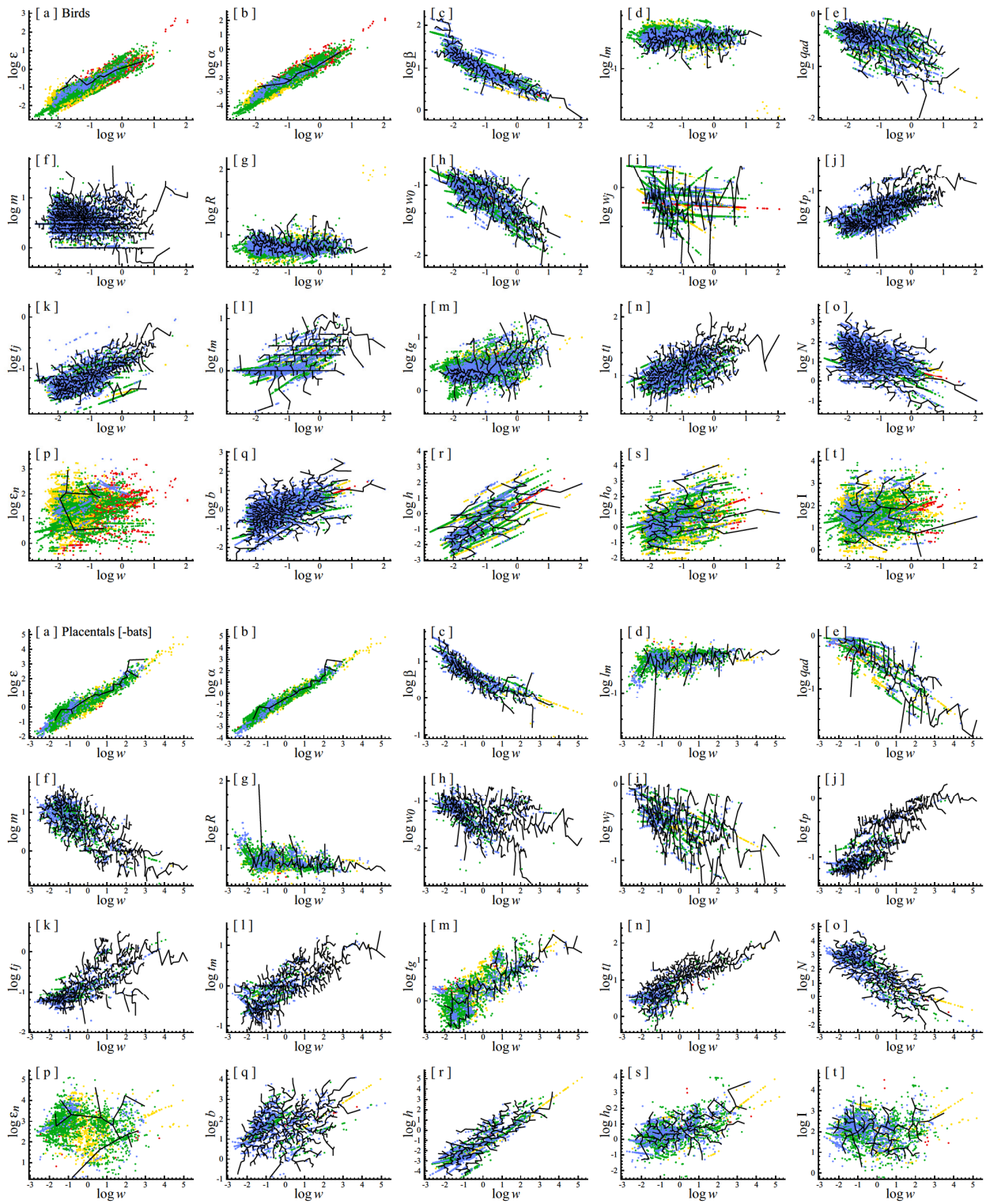
Figure 3: Allometric plots. The relationships between body mass and different traits on double logarithmic scale for birds (top four rows) and placentals (minus bats, bottom four rows). The non-overlapping black lines connect data, and the coloured dots are estimates at different levels. Estimator levels: data (black), genus (blue), family (green), order (yellow), and class (red); with points of the latter sitting on top of the former.
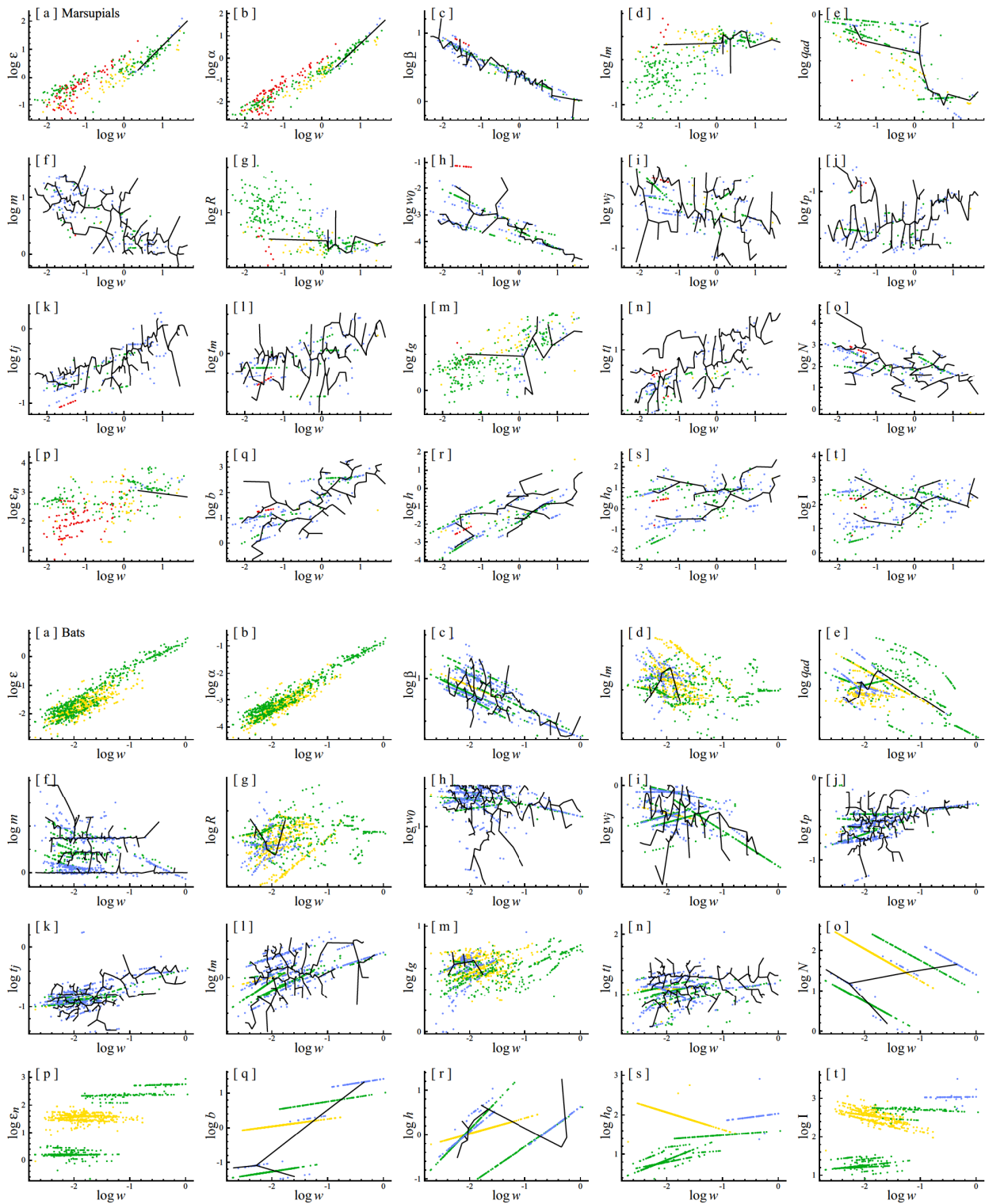
Figure 4: Allometric plots. The relationships between body mass and different traits on double logarithmic scale for marsupial mammals (top four rows) and bats (minus bats, bottom four rows). The non-overlapping black lines connect data, and the coloured dots are estimates at different levels. Estimator levels: data (black), genus (blue), family (green), order (yellow), and class (red); with points of the latter sitting on top of the former.

Trait	w	$\tilde{w}_0$	$\tilde{w}_j$	$\tilde{w}_f$	t_p	t_j	t_m	t_r	t_g	t_l	l_m	p_{ad}	m_b	m_f	R
Unit	kg	-	-	-	y	y	y	y	y	y	t_m^{-1}	y^{-1}	-	y^{-1}	t_r^{-1}
Lesser Long-tailed Shrew Tenrec *Microgale longicaudata*	a:c:d / .0078	.42 / .12	.0098 / .39	.17 / .4	.15 / .13	.19 / .079	1.1 / .89	1.4 / 1.4	1.8 / 2	1.8 / 2.3	1.4 / .23	.82 / .3	.14 / 4.2	— / 1.4	1.4 / 8.5
Philippine Colugo *Cynocephalus volans*	a:c:d:e / 1.3	c:d / .029	d / .3	.17 / .4	c:d / .23	c:d / .53	.78 / 1.2	1.3 / 2.8	1.5 / 3.6	d / 18	1.4 / .53	.82 / .64	c:d:e / 1	.58 / 1.3	1.4 / 3.7
Mas Night Monkey *Aotus nancymai*	a:c:d / .79	.053 / .11	— / .35	— / .11	.038 / .37	.62 / .29	.014 / 2.4	.69 / 5	.69 / 6.4	d / 11	.71 / .34	.67 / .85	c:d / 1	.16 / 1.2	.71 / 5.8
Southern Silvery Mole-rat *Heliophobius argenteocinereus*	a:c:d / .15	.061	.26 / .25	.17 / .42	c:d / .24	.37 / .093	.25 / 1.2	.56 / 2.3	.62 / 3.1	.62 / 3.5	.56 / .27	.51 / .57	c:d:e / 2.3	.56 / 1.4	.56 / 7.3
Saxicoline Deermouse *Peromyscus gratus*	a:c:d / .027	d / .085	d / .38	.17 / .34	d / .078	d / .082	d / .19	.5 / .46	.5 / .49	d / 5.4	.5 / .37	.5 / .21	d / 3.4	d / 3.4	.5 / 5.4
Manus Island Mosaic-tailed Rat *Melomys matambuai*	a:c:d / .12	.73 / .053	.34 / .25	.3 / .27	.26 / .092	d / .055	.3 / .53	.94 / 1.3	.99 / 1.5	— / 4.4	1.1 / .43	.67 / .77	d / 2.1	.6 / 1.8	1.1 / 4.6
Luzon Shrew Mouse *Crunomys fallax*	a:d / .037	.46 / .077	.38 / .32	.3 / .27	.23 / .072	.31 / .063	.3 / .27	.82 / .54	.87 / .64	.67 / 3.5	1 / .3	.5 / .15	.43 / 3.4	.39 / 3.6	1 / 6.6
Southern Golden Bat *Mimon bennettii*	a:c:d / .017	.62 / .16	.13 / .62	.46 / .52	.28 / .36	.91 / .13	.27 / .84	.54 / 3.3	.6 / 3.8	.5 / 12	.54 / .61	.46 / .7	d / 1	d / 1	.54 / 3.3
Altai Mountain Weasel *Mustela altaica*	a:c:d / .18	.35 / .02	.89 / .43	— / .37	c:d / .11	c:d / .15	.37 / .49	.37 / .99	.52 / 1.1	.21 / 10	.37 / .33	— / .42	c:d / 5.6	d / 1.1	.37 / 6.1
Steppe Polecat *Mustela eversmanii*	a:c:d:e / 1.3	c:d / .0062	.89 / .31	— / .37	c:d / .11	c:d / .14	c:e / .94	1	c:e / 1.6	d / 14	c:d:e / .23	— / .67	c:d:e / 8.3	c:d:e / 1	c:d:e / 8.6
Bar-shouldered Dove *Geopelia humeralis*	b:d:hz / .13	.39 / .056	.24 / .81	— / .32	.031 / .042	— / .045	.63 / .63	.92 / 1.2	1.1 / 1.5	.016 / 17	1 / .37	.47 / .61	d:i / 2	.48 / 2.4	1 / 5.5
Seram Mountain-pigeon *Gymnophaps stalkeri*	b:d / .33	.39 / .037	.24 / .81	— / .32	.15 / .044	.32 / .06	.63 / .93	.92 / 3	1.1 / 3.6	.53 / 17	1 / .35	.47 / .67	— / 1	.48 / 1.9	1 / 5.8
White-headed Woodpecker *Leuconotopicus albolarvatus*	b:d / .061	— / .064	.24 / .82	— / .47	d / .038	d / .071	.26 / .83	.64 / 1.1	.69 / 1.6	.048 / 16	.64 / .4	.58 / .76	d:i / 4.4	k / 1	.64 / 5
Malabar Parakeet *Nicopsitta columboides*	b:d / .086	.13 / .045	— / .91	.36 / .51	.13 / .061	.25 / .11	.41 / 1.3	.61 / 1.4	.73 / 2.3	— / 13	.61 / .32	.44 / .74	d:i / 4.4	.072 / 1	.61 / 6.2
Grey-headed Broadbill *Smithornis sharpei*	b:d / .038	.25 / .076	.18 / .77	.27 / .51	.16 / .04	.27 / .046	.21 / 1.1	.45 / 2.8	.5 / 3.5	.4 / 11	.45 / .36	.4 / .64	d:i / 2	k / 1	.45 / 5.5
Band-tailed Antshrike *Thamnophilus melanothorax*	b:d / .032	.25 / .08	— / .78	.27 / .51	.019 / .041	.093 / .031	.21 / 1.1	.41 / 2.7	.46 / 3.4	— / 11	.42 / .36	.35 / .73	.087 / 2.1	k / 1	.42 / 5.6
Lineated Woodcreeper *Lepidocolaptes albolineatus*	b:d / .02	.25 / .092	.18 / .82	.27 / .51	— / .039	.042 / .05	.21 / 1	.42 / 2.7	.46 / 3.3	.019 / 5.4	.52 / .33	.17 / .63	.32 / 2.3	k / 1	.52 / 6
Crested Drongo *Dicrurus forficatus*	b:d / .047	.25 / .07	.18 / .76	.27 / .51	.016 / .045	.016 / .039	.21 / 1.1	.45 / 2.3	.5 / 3.1	.028 / 7.9	.45 / .31	.4 / .66	d:i / 2.8	k / 1	.45 / 6.4
Tickells Leaf-warbler *Phylloscopus affinis*	b:d / .0065	.024 / .11	.18 / .93	.13 / .52	.098 / .035	.12 / .036	.026 / .93	.18 / 1.7	.18 / 2.3	.65 / 6.2	.18 / .3	.18 / .41	d:i / 3.9	k / 1	.18 / 6.6
Przevalskis Rosefinch *Urocynchramus pylzowi*	b / .029	.25 / .083	.18 / .8	.27 / .51	.16 / .039	.27 / .044	.21 / 1.1	.64 / 2	.67 / 2.7	.4 / 10	.78 / .3	.4 / .62	.38 / 2.7	.24 / 1.2	.78 / 6.6

Table 4: Trait estimates of growth and demography for 20 randomly chosen mammals and birds. Estimator levels: data (black), genus (blue), family (green), order (yellow), and class (red). Superscript letters are data references (see SI on data references) and superscript values the sd of the log of data over their predicted cross-validation values for the data of the estimator (no sd for single-data estimators).

This body mass variation is selected from underlying variation in net energy mainly, where the population dynamic feedback selects net energy from reproduction to body mass—and vice versa—to maintain the population dynamic growth that generates the invariant level of interference competition that is selected by the selection attractor of mass (for details on the mechanism, see e.g. Witting 1997). This selection predicts the dependence of mass (w) on net energy (ϵ) as an allometric relation where $w \propto \epsilon^{4/3}$ for a two dimensional foraging ecology (Witting 2017a), with the proportional relation ($w \propto \epsilon$) being between body mass and net energy on the per-generation timescale of natural selection.

The $\epsilon^{4/3}/w$ ratios of the expected 95% range in body mass (calculated from the $\epsilon^{4/3}$ allometry given the 95% range in net energy) over the observed 95% body mass range are 1.30, 1.22, 0.93, and 1.68 for BPMB. This lack of a 100% match reflects at least to some degree body mass deviations that are selected from allometrically uncorrelated variation in the survival of adults and offspring.

The efficiency by which a species allocates net energy into body mass is reflected in the w/ϵ ratio. The medians of this ratio are 0.62, 0.23, 0.34, and 0.67kg/W for BPMB, showing that birds and bats are selected for a more efficient conversion of net energy to mass relative to placentals and marsupials. We will take a closer look at reasons for these differences when we examine

Trait	w	α	$\underline{\beta}$	β	ϵ	$\tilde{\epsilon}_g$	N	b	ϵ_n	h	h_o	v	I
Unit	kg	J	$\frac{\text{W}}{\text{kg}}$	$\frac{\text{W}}{\text{kg}}$	W	-	$\frac{1}{\text{km}^2}$	$\frac{\text{kg}}{\text{km}^2}$	$\frac{\text{W}}{\text{km}^2}$	km^2	-	-	-
Lesser Long-tailed Shrew Tenrec *Microgale longicaudata*	[a:c:d] .0078	$^{2.3}$ .0015	$^{.31}$ 16	$^{.31}$ 33	$^{2.2}$ .049	$^{2.3}$ 5.7	$^{2.1}$ 1100	$^{2.1}$ 8.3	$^{3.1}$ 300	$^{3.7}$ .00036	$^{4.3}$ .39	$^{3.8}$ 150	$^{4.3}$ 59
Philippine Colugo *Cynocephalus volans*	[a:c:d:e] 1.3	$^{2.3}$ .25	$^{.43}$ 2.8	$^{.47}$ 7.9	$^{2.2}$ 1.9	$^{2.3}$ 5.6	$^{1.9}$ 40	$^{1.9}$ 50	$^{2.9}$ 430	$^{2.3}$ .19	^{3} 7.5	$^{2.4}$ 20	^{3} 150
Mas Night Monkey *Aotus nancymai*	[a:c:d] .79	$^{.94}$ .2	$^{—}$ 2.6	$^{—}$ 6	$^{.94}$ 1.2	$^{.94}$ 4.4	[c:ad] 32	[c:ad] 25	$^{.94}$ 170	$^{—}$ .052	[c:ad] 1.7	$^{—}$ 15	25
Southern Silvery Mole-rat *Heliophobius argenteocinereus*	[a:c:d:e] .15	$^{1.5}$ .02	[c:e:f] 4.8	$^{1.5}$ 16	$^{1.5}$ .33	$^{1.5}$ 7.8	[c:ad] 5800	[c:ad] 850	$^{1.5}$ 15000	[nk:nl] .00017	[c:ad:nk:nl] 1	[nk:nl] 480	[nk:nl] 480
Saxicoline Deermouse *Peromyscus gratus*	[a:c:d] .027	$^{1.2}$ .012	$^{.21}$ 8.8	$^{.21}$ 21	$^{1.2}$ .24	$^{1.2}$ 2.9	$^{.97}$ 990	$^{.97}$ 27	$^{1.5}$ 690	$^{1.2}$ .0038	$^{1.5}$ 3.7	$^{1.2}$ 57	$^{1.5}$ 210
Manus Island Mosaic-tailed Rat *Melomys matambuai*	[a:c:d] .12	$^{1.6}$ .017	$^{.37}$ 4.9	$^{.37}$ 17	$^{1.5}$ .29	$^{1.6}$ 7.2	$^{—}$ 460	$^{—}$ 54	$^{1.6}$ 970	$^{1.8}$ .0031	$^{1.8}$ 1.4	$^{1.8}$ 100	$^{1.8}$ 150
Luzon Shrew Mouse *Crunomys fallax*	[a:d] .037	$^{1.4}$ .017	$^{.37}$ 6.9	$^{.37}$ 24	$^{1.4}$ .4	$^{1.4}$ 2.7	$^{1.4}$ 870	$^{1.4}$ 32	^{2} 940	$^{1.8}$ .0021	$^{2.3}$ 1.8	$^{1.8}$ 100	$^{2.3}$ 180
Southern Golden Bat *Mimon bennettii*	[a:c:d] .017	$^{3.7}$ .00053	$^{.25}$ 9.3	$^{.28}$ 32	$^{3.7}$ .017	$^{3.7}$ 33	^{3} 72	^{3} 1.2	$^{4.8}$ 40	$^{1.2}$ 1.3	$^{3.2}$ 92	$^{1.3}$ 3.7	$^{3.2}$ 340
Altai Mountain Weasel *Mustela altaica*	[a:c:d] .18	$^{1.1}$ .038	$^{.31}$ 9.9	$^{.32}$ 26	$^{1.1}$ 1	$^{5.1}$ 5.1	$^{.68}$ 7	$^{.68}$ 1.2	$^{1.3}$ 36	$^{1.2}$ .74	$^{1.4}$ 5.2	$^{1.3}$ 13	$^{1.4}$ 66
Steppe Polecat *Mustela eversmanii*	[a:c:d:e] 1.3	^{1} .48	$^{.31}$ 3.8	$^{.32}$ 12	$^{.94}$ 5.6	^{1} 3.3	$^{.68}$ .84	$^{.68}$ 1.1	$^{1.2}$ 15	$^{1.2}$ 1.5	$^{1.4}$ 1.3	$^{1.3}$ 11	$^{1.4}$ 14
Bar-shouldered Dove *Geopelia humeralis*	[b:d:hz] .13	$^{1.1}$ .018	$^{.073}$ 5.1	$^{.073}$ 10	$^{1.1}$ .18	$^{1.1}$ 7.8	$^{—}$ 14	$^{—}$ 1.8	$^{1.1}$ 20	$^{5.1}$ 3.2	$^{5.1}$ 45	$^{5.1}$ 2	$^{5.1}$ 93
Seram Mountain-pigeon *Gymnophaps stalkeri*	[b:d] .33	$^{1.2}$ .02	$^{.16}$ 4.9	$^{.16}$ 9.8	$^{1.2}$ .2	$^{1.2}$ 17	$^{—}$ 7.2	$^{—}$ 2.4	$^{1.2}$ 24	$^{5.1}$ 12	$^{5.1}$ 88	$^{5.1}$ 1.6	$^{5.1}$ 140
White-headed Woodpecker *Leuconotopicus albolarvatus*	[b:d] .061	$^{.92}$ .0057	$^{.44}$ 15	$^{.44}$ 19	$^{.81}$ .11	$^{.92}$ 11	$^{.73}$ 7.6	$^{.73}$ .47	$^{1.2}$ 9.1	$^{—}$ .64	$^{.73}$ 4.9	$^{.44}$ 5.8	$^{.85}$ 28
Malabar Parakeet *Nicopsitta columboides*	[b:d] .086	$^{2.2}$ .011	$^{.32}$ 9.7	$^{.23}$ 18	$^{2.2}$ .2	$^{2.2}$ 8.3	$^{1.5}$ 17	$^{1.5}$ 1.5	$^{2.7}$ 29	$^{—}$ .013	$^{1.5}$ .22	$^{.23}$ 47	$^{1.5}$ 11
Grey-headed Broadbill *Smithornis sharpei*	[b:d] .038	$^{1.7}$ .00087	$^{.27}$ 14	$^{.29}$ 38	$^{1.6}$ .033	$^{1.7}$ 44	$^{1.5}$ 18	$^{1.5}$ .68	$^{2.2}$ 26	$^{1.5}$ .082	$^{2.1}$ 1.5	$^{1.5}$ 26	$^{2.1}$ 38
Band-tailed Antshrike *Thamnophilus melanothorax*	[b:d] .032	$^{1.6}$ .00064	$^{—}$ 14	$^{—}$ 41	$^{1.6}$ .026	$^{1.6}$ 50	[a d] 2.5	[a d] .08	$^{1.6}$ 3.3	$^{1.5}$ .069	$^{1.5}$ .17	$^{1.5}$ 27	$^{1.5}$ 4.8
Lineated Woodcreeper *Lepidocolaptes albolineatus*	[b:d] .02	$^{1.6}$ .0006	$^{—}$ 13	$^{—}$ 35	$^{1.6}$ .021	$^{1.6}$ 34	[a d] 5.5	[a d] .11	$^{1.6}$ 4	$^{1.5}$ .045	$^{1.5}$ .25	$^{1.5}$ 24	$^{1.5}$ 5.9
Crested Drongo *Dicrurus forficatus*	[b:d] .047	$^{1.6}$ .0015	$^{.27}$ 13	$^{.29}$ 35	$^{1.6}$ .053	$^{1.6}$ 32	[a d] 57	[a d] 2.7	$^{1.6}$ 96	$^{1.5}$ .1	$^{1.5}$ 5.8	$^{1.5}$ 24	$^{1.5}$ 140
Tickells Leaf-warbler *Phylloscopus affinis*	[b:d] .0065	$^{.76}$ .00026	$^{.015}$ 21	$^{.015}$ 59	$^{.76}$ .015	$^{.76}$ 26	$^{1.6}$ 66	$^{1.6}$ .43	$^{1.8}$ 26	$^{—}$ .026	$^{1.6}$ 1.7	$^{.015}$ 30	$^{1.6}$ 51
Przevalskis Rosefinch *Urocynchramus pylzowi*	[b] .029	$^{1.8}$ .001	$^{.27}$ 15	$^{.29}$ 43	$^{1.8}$ .044	$^{1.8}$ 28	$^{1.5}$ 20	$^{1.5}$ .56	$^{2.3}$ 24	$^{1.5}$ .062	$^{2.1}$ 1.2	$^{1.5}$ 29	$^{2.1}$ 36

Table 5: Trait estimates of the energetics and population ecology for 20 randomly chosen mammals and birds. Estimator levels: data (black), genus (blue), family (green), order (yellow), and class (red). Superscript letters are data references (see SI on data references) and superscript values the sd of the log of data over their predicted cross-validation values for the data of the estimator (no sd for single-data estimators).

the demographic traits below but let us first examine how the different taxa generate net energy.

With the net energy of a species following from the $\epsilon = \alpha\beta$ product between resource handling (α) and metabolic pace (β), the inter-specific variation in net energy and body mass reflects underlying variation in resource handling and mass-specific metabolism. As mass-specific metabolism in birds and mammals approach Kleiber (1932) scaling with allometric exponents around $-1/4$, the 95% range of mass-specific metabolism should cover approximately 25% of the corresponding range in body mass. With the actual β/w ratios of the 95% range being 0.42, 0.28, 0.29, and 0.29 for BPMB this holds approximately for most taxa, ex-

cept that especially the metabolic estimates of birds have more variation than expected from Kleiber scaling alone.

As the $-1/4$ power decline in mass-specific metabolism with an increase in mass is selected as a secondary mass-rescaling that is imposed by the selection of mass (Witting 2017a), the primary contributor to the selected variation in body mass is the underlying variation in resource handling, reflecting variation in the ways that species handle their resources as well as variation in the density of resources. This downscaling of mass-specific metabolism ($\beta \propto w^{-1/4}$) during the selection of mass generates a decline in net energy in physical time ($\epsilon = \alpha\beta \propto w^{-1/4}$ given constant α), but

Trait	w	ϵ	$\underline{\beta}$	α	m	t_r	l_m	q_{ad}	R	N	b	h	h_o	ι
Unit	g	W	$\frac{\text{W}}{\text{kg}}$	J	y^{-1}	y	t_m^{-1}	y^{-1}	t_r^{-1}	$\frac{1}{\text{km}^2}$	$\frac{\text{kg}}{\text{km}^2}$	km^2	-	-
Birds	$36^{58}_{2.2}$	$.058^{0.086}_{2.2}$	$13^{11}_{.93}$	$.0016^{0.0031}_{3.1}$	$3.3^{3.3}_{.79}$	$2^{2}_{.6}$	$.32^{0.3}_{.33}$	$.36^{0.32}_{.61}$	$6.3^{6.6}_{.33}$	14^{13}_{2}	$.73^{0.77}_{2.2}$	$.084^{0.18}_{3.1}$	$1.8^{2.4}_{2.9}$	$1^{-}_{1.9}$
Plac.	150^{58}_{4}	$.65^{0.3}_{3.3}$	$4.9^{7.2}_{1.1}$	$.042^{0.015}_{4.3}$	$6.5^{8.1}_{1.5}$	$1.2^{0.84}_{1.5}$	$.32^{0.29}_{.38}$	$.6^{0.64}_{1.1}$	$6.2^{6.8}_{.38}$	$350^{480}_{3.7}$	$41^{28}_{2.5}$	$.0042^{0.0029}_{4.8}$	$1.9^{2.6}_{2.6}$	2.5^{-}_{2}
Mars.	$340^{58}_{2.9}$	$.99^{0.37}_{2.1}$	$3^{4.8}_{.84}$	$.093^{0.021}_{3.1}$	$4.7^{7.6}_{1.3}$	$1.5^{1.2}_{.88}$	$.3^{0.21}_{.59}$	$.59^{0.65}_{.69}$	$6.6^{9.4}_{.59}$	$100^{180}_{1.8}$	$23^{11}_{2.7}$	$.024^{0.0062}_{3.1}$	$4.6^{1.2}_{3}$	$2.4^{-}_{2.3}$
Bats	$14^{58}_{1.8}$	$.021^{0.12}_{2.3}$	$7.7^{5.7}_{.52}$	$.00065^{0.0041}_{2.4}$	$1.3^{1.3}_{.44}$	$3.4^{3.6}_{.41}$	$.42^{0.41}_{.23}$	$.27^{0.24}_{.4}$	$4.7^{4.9}_{.23}$	$49^{36}_{1.7}$	$1.1^{2.1}_{2.6}$	$1.1^{1.3}_{1}$	$65^{48}_{1.5}$	$3.1^{-}_{1.8}$

Table 6: The inter-specific medians of selected traits covering all PDHL models for birds, placentals, marsupials, and bats. Superscripts are the expected trait values of 58g body masses (the mean of median bird & median mammal mass), and subscripts the 95% order of magnitude range of the inter-specific distributions (calculated for $I = e^{\iota}$ for interference).

it maintains net energy on the per-generation timescale of natural selection ($\epsilon t_r \propto w^0$ given constant α) because it includes a corresponding dilation ($t_r \propto 1/\beta \propto w^{1/4}$) of natural selection time. Thus, when other things are equal, the body mass within a taxon should be selected in proportion to resource handling ($w \propto \alpha$).

The dependence of mass on resource handling is reflected in the α/w ratio, with the ratios of the 95% ranges of the inter-specific distributions being 1.41, 1.07, 1.07, and 1.33 for BPMB. These ratios are close to the other-things-being-equal-value of unity for placentals and marsupials. The larger α/w ratio for birds reflects—at least to some degree—a smaller (-0.33; se:0.01; Witting 2023a) than expected ($-1/4$) allometric exponent for mass-specific metabolism. This stronger decline relative to Kleiber scaling implies an additional decline in the pace of handling with increased mass, implying a stronger than proportional dependence of mass on resource handling as the $\alpha\beta$ product provides the net energy that is selected into mass.

With a metabolic scaling exponent of -0.21 (se:0.02; Witting 2023a), the larger than expected α/w ratio for bats have another cause. Where the scaling exponent for adult mortality is close to the $-1/4$ expectation for birds, placentals, and marsupials, it is only -0.07 (se:0.08) for bats (Witting 2023a). This reduced decline in mortality with increased mass implies a reduced increase in mass with increased resource handling (see Demography section below), and thus a α/w ratio that is larger than otherwise expected.

The stronger metabolic scaling in birds may reflect a diversification that increases as a taxon evolves through time (Witting 2018, 2023a), with the primary selection of metabolism accelerating more in smaller species as they are selected over a larger number of generation than larger species. This deviation from a linear metabolic allometry is found also in terrestrial placentals (Kolokotrones et al. 2010), but not in marsupials which have close to perfect Kleiber scaling with

an allometric exponent of -0.25 (MacKay 2011). This agrees with the above α/w ratio of unity for marsupials, while the close to unity value for placentals is somewhat confounded as it is a joint measure for both two-dimensional (2D) and three-dimensional (3D) ecological systems, with the estimated metabolic exponent of placentals being -0.29 for 2D and -0.14 for 3D (Witting 2023a).

To examine the different ways the different taxa generate net energy, let us compare the median β/α ratios. These are 8100, 120, 32, and 12000/kg s for BPMB, which means that metabolic pace is much more important for the generation of net energy in bats and birds than in placentals and marsupials. If we correct for mass and compare the corresponding β/α ratios at the 58g intercept, we find a less extreme but similar difference (3500, 480, 230, & 1400). This reflects a resource handling in birds and bats that is only 21% and 27% of the corresponding resource handling in placentals, with mass-specific metabolism in birds and bats at 58g being 153% and 79% of the corresponding metabolism in placentals. Hence, the importance of metabolism in bats is due to their much smaller size than most placentals, while the importance in birds reflects also a higher primary selected level of metabolism. The low β/α ratio in marsupials reflects both a mass-specific metabolism that is only 67% of the metabolism in placentals at the 58g intercept, and a resource handling at 58g that is 140% of handling in placentals.

Demography: With demographic parameters like m, t_m, t_r, and q_{ad} being yearly rates or ages/periods they tend to scale inversely with mass-specific metabolism, with many of the allometric exponents for terrestrial birds and mammals being around 1/4 (Witting 1995, 2023a). The 95% range of the inter-specific variation are thus as expected about similar to the corresponding range for mass-specific metabolism, with the ratio of the average range of m, t_m, t_r, and q_{ad}

over the range of β being 0.69, 1.2, 1.1, and 0.87 in BPMB.

The population dynamic feedback selection of mass selects a balance between the demographic traits that maintains the population dynamic growth that generates the intra-specific interference competition of the selection attractor on body mass. This balance depends on the survival of offspring and adults, and this affects the conversion of net energy into body mass (as measured by individual mass).

The selected body mass reflects the available net energy per offspring, with the energy mass conversion efficiency being proportional to the $t_r\epsilon/R$ ratio of lifetime net energy ($t_r\epsilon$) over lifetime reproduction (R). And with lifetime reproduction being inversely related to offspring survival to maturity ($R = 2/l_m$ from $\lambda = l_m R/2 = 1$), and the reproductive period being inversely related to adult mortality ($t_r = \min[4/mp_{ad}^{t_m}, 1/(1 - p_{ad})]$), the efficiency declines with a smaller mass being selected if offspring and/or adult mortality increases. An increase in offspring mortality selects for a decline in mass to produce more offspring from the same amount of energy to obtain the same number of surviving offspring. And an increase in adult mortality selects for a decline in mass to match the decline in net energy available for the production of the selected number of offspring per reproductive period (that maintains the $\lambda = l_m R/2 = 1$ balance at the abundance that generates the interference competition of the selection attractor on mass).

These relations are evident in the life history differences among the four taxa. With median offspring survival (l_m) in bats being 134%, and median adult survival 151% of the average median offspring and adult survival in birds, placentals, and marsupials, bats have the most efficient conversion of net energy to mass, with a median w/ϵ conversion ratio of 0.67kg/W, which is 169% of the average median across the other three taxa. This is reflected in the lowest median lifetime reproduction of $4.7/t_r$, the longest median reproductive period of 3.4y, and the lowest median annual reproduction of 1.3/y.

Following bats, birds have the second highest median w/ϵ conversion efficiency of 0.62kg/W, with marsupials having the third highest (0.34kg/W), and placentals the lowest (0.23kg/W) conversion efficiency. This stepwise decline reflects a decline in the median reproductive period (2y, 1.5y, 1.2y) driven primarily by an increase in median adult mortality (0.36, 0.59, 0.6). Yet, birds, marsupials, and placentals have about similar median survival of offspring to reproductive maturity (0.32, 0.3, 0.32) and similar median lifetime reproduction ($6.3/t_r$,

$6.6/t_r$, $6.2/t_r$). The mortality driven decline in the reproductive period across the three taxa is thus selected into a corresponding increase in median yearly reproduction (3.3/y, 4.7/y, 6.5/y) following the $R = mt_r$ relation.

Ecology: For the ecological traits there are only few data for bats, and I will not include them in the comparison. For the remaining three taxa let us examine the 95% range for abundance (N), biomass (b), home range (h), and home range overlap (h_o) relative to the expected range from the variation in body mass given the allometric relations $N \propto w^{-3/4}$, $b \propto w^{1/4}$, $h \propto w^1$, & $h_o \propto w^{1/4}$ (I do not include ϵ_n and ι as these are predicted invariant of w). These ratios show that the average observed range in N, b, h, and h_o are 1.08, 1.88, 1.23, and 2.17 times the expected range. These numbers indicate a large overdispersion in b and h_o relative to the allometric expectations, which may reflect not only additional ecological variation but also increased estimation uncertainty for ecological traits.

When it comes to between taxa differences there is for most ecological traits a very large difference between birds and mammals (especially placentals). The median abundance, biomass, and resource consumption of placental populations are 25, 56, and 30 times the corresponding medians for birds, and the median home range of placentals is only 5% of the median of birds. These differences remain pronounced when corrected for mass, where the median intercepts for abundance and biomass in placentals are 37 times the medians for birds, while the median intercept for placental home range is only 1.6% of the median intercept in birds. These large ecological differences between birds and mammals are in sharp contrasts to the median home range overlap, which is essentially identical between the two taxa (1.8 in birds vs. 1.9 in placentals).

The similar home range overlap in birds and mammals indicates that the spatial packing of home ranges plays a central role in the joint natural selection of the life histories and population dynamic ecology as a whole. This is in line with population dynamic feedback selection, where it is the density-dependent trade-off between the local resource exploitation of individuals and the interactive competition between individuals that selects a home range overlap that optimises the individual foraging ecology, with the spatial dimensionality of the ecological packing of home ranges constraining the exponents of body mass allometries (Witting 1995, 2017a, 2023a).

The level of interference competition that is selected by the spatial packing of home ranges is the main selec-

tion attractor of population dynamic feedback selection, known as a competitive interaction fixpoint (Witting 1997). This attractor reflects a process where the population dynamic demography, density regulated abundance, and associated foraging ecology are feedback selected to a balance where they generate a level of interactive competition that is invariant of the selected body mass and pre-defined by the selection attractor of the competitive interaction fixpoint.

Dependent upon the overall constraints on the selection of mass, the level of interference competition at the competitive interaction fixpoint may differ (Witting 2002, 2008, 2017b). The theoretical ratio in the ι-level of interference for the selection attractor of an exponentially increasing body mass over the attractor of a stable mass, e.g., is $7/3 \approx 2.3$ given a two-dimensional packing of home ranges. This is close to the observed values of 2.5 and 2.4 for the placental/bird and marsupial/bird ratios of the median ι-estimates in Table 6.

Apart from the elevated interference competition—and associated increase in population abundance, biomass, and population energy consumption—that is necessary for the selection of an exponential increase in body mass, the feedback selection mechanisms for a stable and increasing body mass are similar selecting no obvious difference in the physiology and demography (while differences are selected in the reproducing unit; Witting 2002). Hence, the median ecological differences, and relative demographic similarities, between birds and mammals (excluding bats) indicate that mammals are predominately selected for an increase in mass while birds are selected for a stable mass.

3.3 Population dynamics

This section illustrates how the 16,123 equilibrium life history models are easily extended into age-structured population dynamic simulations. This is exemplified by eight models that explain a diverse range of population dynamic timeseries.

The population dynamics of a species depend on the age-structured demography that defines the timescale of the dynamics, and on the population dynamic regulation that defines not only the bounds on abundance but also the properties of the dynamics, let it be monotonic growth, damped to stable population cycles, fluctuating, or chaotic dynamics.

While regulation is relatively easily estimated from timeseries of abundance estimates, this is not the case for the age-structured demography. It is thus essential that the latter is available from other sources, as the life history models in this paper. When these age-

structured models are simulated with no regulation, they project a stable population in time.

Given widespread evidence for eco-evolutionary dynamics (e.g., Thompson 1998; Sinervo et al. 2000; Hairston et al. 2005; Coulson et al. 2011; Turcotte et al. 2011a,b; Bell 2017; Hendry 2017; Brunner et al. 2019), I follow Witting (2000b, 2013) and maintains the structure of population dynamic feedback selection in my population dynamic simulations. This means that I add natural selection regulation on top of density regulation. As described in Appendix C, in addition to the inclusion of a density regulation parameter (γ) that regulates the growth rate as a function of the density-dependent environment, this includes also a selection regulation parameter (γ_ι) that accelerates the population dynamic growth below the equilibrium abundance and decelerates population growth above. Following Witting (2023c), I use *i*) maximum likelihood statistics to estimate the two regulation parameters (and the equilibrium and initial abundance, as well as an initial measure of competitive quality) and *ii*) the Akaike information criterion (AIC, Akaike 1973) to determine if there is additional evidence for a change in equilibrium abundance or catastrophic mortality in a specific year.

The eight examples of fits to timeseries of abundance estimates are shown in Fig. 5. For these, I estimate that about 20% to 80% of total regulation is caused by selection, as measured by the $\gamma_\iota/(\gamma + \gamma_\iota)$ ratio. This generates a cyclic/over-compensatory dynamics that cannot be explained by density regulation alone. The over-compensation is illustrated by the growth of European Otter (*Lutra lutra*, from Sulkava 2006; LPI 2022) in Finland. The Eurasian Pygmy Owl (*Glaucidium passerinum*, from Knaus et al. 2022) in Switzerland illustrates that populations that are both density and selection regulated have the ability to decline for longer periods below the equilibrium abundance, and to increase for longer periods above the equilibrium. Pure density regulated populations will typically only decline above the equilibrium and increase below.

Many birds that live in the farmlands of Europe have declined more or less continuously since systematic monitoring was established in several countries in the 1970th and 1980th (Gregory et al. 2019; PECBMS 2022). This is illustrated by Eurasian Skylarks (*Alauda arvensis*, from DOF 2022) in Denmark and Yellowhammers (*Emberiza citrinella*, from SFT 2022) in Sweden. The best AIC-selected models estimate that Skylark habitats in Denmark and Yellowhammer habitats in Sweden have fragmented and deteriorated by 64% and 80% since the middle of the 1970th.

Where many species suffer, others benefit from habi-
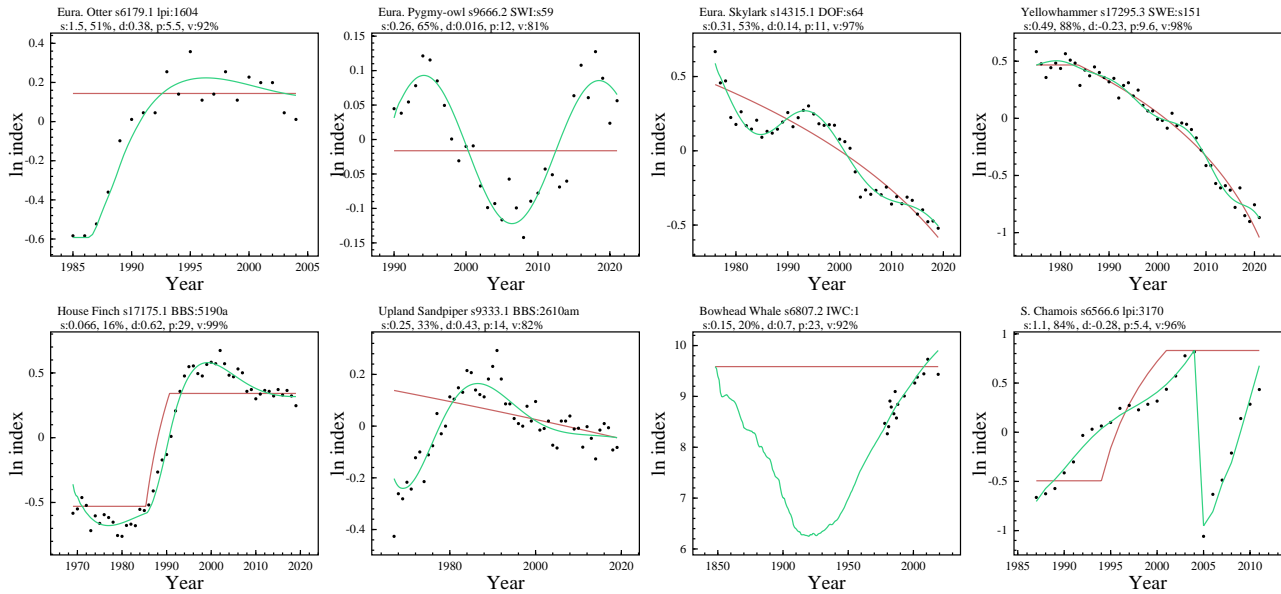
Figure 5: Age-structured population dynamic models fitted to timeseries of abundance estimates (see Section 3.3 for details). Dots are index series of abundance, red lines the estimated equilibria, and green curves the model trajectories. s:γ_ι & $\gamma_\iota/(\gamma_\iota + \gamma)$ in %; d:damping ratio; p:period in generations; v:explained variance.

tat changes imposed by humans. Being originally a bird of the western Unites States and Mexico, House Finches (*Haemorhous mexicanus*) established themselves in human-altered habitats throughout the Unites States and southern Canada following a small release on Long Island in the 1940th. Across the mid-west the population was relatively stable from 1970 to 1980, followed by a large increase driven by a three-fold increase in equilibrium (most likely expansion into new habitats), according to the best AIC selected model run on data compiled (Witting 2023b) from BBS (2022).

A strong population increase need not necessarily reflect improved conditions. Being a grassland species native to the prairies of Unites States and Canada, the Upland Sandpiper (*Bartramia longicauda*) is another species that is vulnerable to habitats lost to agriculture with an increased use of pesticides. Based on the best AIC selected model run on BBS (2022) data compiled by Witting (2023b), from about 1970 to 1990 Upland Sandpipers recovered by an increase of about 50% from a low abundance. Yet, the estimated habitat conditions deteriorated by about 20% from 1970 to 2020, with the species declining by about 20% from 1990 to 2020.

A longstanding threat to many species is direct anthropogenic removals, with commercial whaling in past centuries causing some of the largest perturbations of natural populations worldwide. The population modelling of these perturbations subtracts the histori-

cal catches from the simulated population, fitting the model trajectory to a relatively short timeseries of recent abundance estimate (Punt and Butterworth 1999; Wade 2002; Witting 2013). The bowhead whale (*Balaena mysticetus*) in the Bering-Chukchi-Beaufort Seas is one example, where the fitted model estimates that the historical catches of about 21,000 bowheads from 1850 to 1950 (data from https://iwc.int) caused a collapse to about 1000 individuals in 1920, less than 7% of the pre-whaling abundance. From about 1910 to 1930 there was a turning point where reduced catches and increased growth (from the relaxed density regulation and selection acceleration of the depleted population) turned the population decline into an increase. With bowheads being reproductively mature around 23 years of age, it took approximately 100 years to recover to a pre-whaling abundance of about 15,000 whales, with today's population continuing to increase.

Population perturbations may also be imposed by natural causes. The Spanish population of Pyrenean Chamois (*Rupicapra pyrenaica*) in Cerdanya-Alt Urgell increased steadily until 2005, where approximately 3,000 died from a border disease virus infection (Marco et al. 2009; data from Lopez-Martin et al. 2013; LPI 2022). This caused the population to collapse by about 80% in a single year. With Chamois being reproductively mature at about 2 years of age the population was almost recovered by 2011.

4   Discussion

The past couple of decades have produced an increased availability of data collections on inter-specific life history variation, generating important resources for studies in ecology and evolution. Where some studies collected data on single traits like body mass (Smith et al. 2004; Dunning 2007), survival (Ziehm et al. 2015), clutch size (Jetz et al. 2008), longevity (Carey and Judge 2002), and population density (Santini et al. 2018), others examined life histories as allometric functions of mass, including traits like metabolism (e.g., McNab 2008; McKechnie and Wolf 2004; Hudson et al. 2013), population density (Damuth 1987; Marquet et al. 1995; Silva et al. 1997), and home range (Tucker et al. 2014; Tamburello et al. 2015; Kelt and Van Vuren 2015).

The larger databases have a broader focus on several traits, with *i*) AnAge documenting longevity and life history traits across the tree of life (De Magalhães and Costa 2009), *ii*) PanTHERIA focussing on life history, ecology, and geographical variation among mammals (Jones et al. 2009), *iii*) Myhrvold et al. (2015) collecting life history data for birds, mammals, and reptiles, *iv*) COMADRE dealing with demographic data and matrix population models that span a rich diversity of the animal kingdom world-wide (Salguero-Gomez et al. 2016), and *v*) AnimalTraits focusing on the connection between body mass, metabolism, and brain size (Herberstein et al. 2022).

Where a common strength of these studies is their focus on data across species and traits, a common weakness is their incompleteness; let it be on the number of species and/or traits included, and on the widespread presence of missing values in the chosen matrix of species and traits. The comparative strength and weakness of my study is the other way around, as my focus on models allows me to estimate all the missing values in a matrix that covers 29 essential life history and ecological traits across 16,123 species of birds and mammals, generating 467,567 estimates in total.

Other strengths of my PDLH models include a trait structure that covers the essential links in population dynamic feedback selection. For each species this provides estimates of the energy flow from the resource to the physiology, over the reproductive output, to the abundance of the population and the associated feeding ecology in overlapping home ranges, generating age-structured demographic models in population dynamic equilibrium. The complete set of single species models form a meta natural selection model, where much of the inter-specific variation in the life history as a whole is explained from underlying variation in a few independent traits. Hence, the meta model allows for evolutionary analyses that are more natural selection informed than traditional analyses.

As frequency-independent selection is usually too rigid for predictions of inter-specific life history covariance (Section 1.1), evolutionary hypotheses on inter-specific variation have traditionally been based on comparative analyses (e.g. Promilsow and Harvey 1990; Harvey and Pagel 1991; Sibly and Brown 2007; Sibly et al. 2012; Dobson 2012; Brown et al. 2018; Burger et al. 2019). These studies identify inter-specific variation that reflects the historical evolution of species, but they lack a formal selection analysis that predicts the inter-specific trait covariance from underlying natural selection causes. Comparative analyses tend to assume that variation in body mass is the primary cause for evolutionary variation in other traits. Yet, the meta model of population dynamic feedback selection shows that body mass is described better as a trait of interactive quality that is selected by the interactive competition that follows from primary selected resource handling and metabolism, combined with ecological variation in resource density and mortality.

Comparative analyses have also described inter-specific variation in relation to a fast–slow continuum (Promilsow and Harvey 1990; Blackburn 1991; Sæther and Bakke 2000; Bielby et al. 2007; Dobson and Oli 2007), or differences in lifestyle (Sibly and Brown (2007); Sibly et al. 2012) and energy use (Brown et al. 2018; Burger et al. 2019). Again, these approaches describe the outcome of evolution, instead of explaining the observed covariance from a mechanistic selection and some underlying variation in independent traits. The same holds for phylogenetic (historical) ecology (e.g. Holder 1983; Brooks and McLennan 1991; McKitrick 1993; Brown 1994; Sibly and Brown 2007; Sibly et al. 2012) that elaborates on observations that go all the way back to pre-Darwinian classification (Linnaeus 1758), where the diversity of life was better accounted for by grouping similar organisms into closely related taxa. Yet, life history differences by phylogenetic distance is the evolutionary outcome of natural selection and other processes of evolution, and not the natural selection cause of life history differences in the first place (Reeve and Sherman 2001).

By aligning life history estimates with the energy flow of population dynamic feedback selection, it is possible to explain much of the life history and population ecological variation from a few natural selection causes. This is illustrated in Section 3.2, where the intra- and inter-taxon variation in birds, placen-

tals, marsupials, and bats are described primarily by the natural selection consequences of variation in resource handling, metabolism, mortality, home range, and abundance. One essential finding indicates that birds may be predominately selected for stable body masses, while mammals are predominantly selected for body masses that increase exponentially on evolutionary timescales. Another example use the life history estimates to illustrate the natural selection of body mass allometries (Witting 2023a). This identifies not only predominant Kleiber scaling, but also allometric deviations imposed by additional variation in mortality and primary selected mass-specific metabolism.

Another strength of the estimated life history models is that they are prepared for an easy extension into age-structured population dynamic simulations. This is illustrated in Section 3.3, with examples showing how a diverse range of population dynamic timeseries are explained by the addition of population dynamic feedback selection on top of traditional density regulated models. A next step is the estimation of age-structured population dynamic models across thousands of population dynamic timeseries (Witting 2023c), allowing for a quantification of the relative importance of regulation by density dependence and natural selection.

My cross-validation of the estimated models found no general estimation bias. Yet, as the majority of the estimated traits are inter-specific extrapolations, and as the underlying data come from many sources, it is essential to keep in mind the uneven distribution of uncertainties. This uncertainty is captured partially by the removal of outliers, filter-adjustments of unlikely values, use of estimators at the lowest taxonomic level with data, and uncertainty measures of estimated traits.

Given these limitations, the value of having complete population dynamic life history models for 11,187 species of birds and 4,936 mammals should not be underestimated. Validated data should always be preferred over model estimates, but life history data are incomplete or missing for most species, and complete population dynamic life history models are needed in many cases. Based on my analysis, I constructed a global library of Bird and Mammal Populations that is freely available for online simulations (at https://mrLife.org). This allows for population dynamic analyses of all species with body mass estimates, including the estimation of expected trajectories given habitats that fragment or improve.

Acknowledgements

References

Akaike H. (1973). Information theory as an extension of the maximum likelihood principle. In: Petrov B. N. Csaki F. (eds). Second International Symposium on Information Theory: Akademiai Kiado, pp 267–281.

Banavar J. R., Maritan A., Rinaldo A. (1999). Size and form in efficient transportation networks. Nature 399:130–132.

BBS (2022). EESC Breding Bird Survey. https://www.mbr-pwrc.usgs.gov/bbs/bbs.html.

Beauchamp G. (2023). Annual apparent survival across species is lower in juvenile than adult birds but has similar ecological correlates. Ibis 165:448–457.

Bell G. (2017). Evolutionary rescue. Ann. Rev. Ecol. Evol. Syst. 48:605–627.

Besbeas P., Freeman S. N., Morgan B. J. T. (2005). The potential of integrated population modelling. Aust. N. Z. J. Stat. 47:35–48.

Besbeas P. T., McCrea R. S., Morgan B. J. T. (2022). Selecting age structure in integrated population models. Ecol. Model. 473:110111.

Bielby J., Mace G. M., Bininda-Emonds O. R. P., Cardillo M., Gittleman J. L., Jones K. E., Orme C. D. L., Purvis A. (2007). The fast–slow continuum in mammalian life history: An empirical reevaluation. Am. Nat. 169.

BirdLife (2022). HBW and BirdLife Taxonomic Checklist v7. BirdLife International, datazone.birdlife.org.

Blackburn T. M. (1991). Evidence for a slow-fast continuum of life-history traits among parasitoid Hymenoptera. Funct. Ecol. 5:65–74.

Brooks D. R. McLennan D. A. (1991). Phylogeny, ecology, and behaviour. University of Chicago Press, Chicago.

Brown J. H., Gillooly A. P., Allen V. M., Savage G. B. (2004). Towards a metabolic theory of ecology. Ecology 85:1771–1789.

Brown J. H., Hall C. A. S., Sibly R. M. (2018). Equal fitness paradigm explained by a trade-off between generation time and ennergy production rate. Nat. Ecol. Evol. 2:262–268.

Brown J. H. Sibly R. M. (2006). Life-history evolution under a production constraint. Proc. Nat. Acad. Sci. 103:17595–17599.

Brown, J. H. & West, G. B., eds (2000). Scaling in biology. Oxford University Press, New York.

Brown J. S. (1994). Review of *Phylogeny, Ecology, and*

Behaviour by D. R. Brooks and D. A. McLennan. J. Mamm. 75:243–246.

Brunner F. S., Deere J. A., Egas M., Eizaguirre C., Raey-maekers J. A. M. (2019). The diversity of eco-evolutionary dynamics: Comparing the feedbacks between ecology and evolution across scales. Funct. Ecol. 33:7–12.

Burger J. R., Hou C., Brown J. H. (2019). Towards a metabolic theory of life history. Proc. Nat. Acad. Sci. 116:26653–26661.

Carey J. R. Judge D. S. (2002). Longevity records. Life spans of mammals, birds, amphibians, reptiles, and fish. Odense University Press, Odense.

Charlesworth B. (1980). Evolution in age-structured populations. Cambridge University Press, Cambridge.

Charnov E. L. (1993). Life history invariants. Some explorations of symmetry in evolutionary ecology. Oxford University Press, New York.

Christiansen F. B. (1991). On conditions for evolutionary stability for a continuously varying character. Am. Nat. 138:37–50.

Coulson T., Macnulty D. R., Stahler D. R., Vonholdt B., Wayne R. K., Smith D. W. (2011). Modeling Effects of Environmental Change on Wolf Population Dynamics, Trait Evolution, and Life History. Science 334:1275–1278.

Damuth J. (1981). Population density and body size in mammals. Nature 290:699–700.

Damuth J. (1987). Interspecific allometry of population density in mammals and other animals: the independence of body mass and population energy-use. Biol. J. Linnean Society. 31:193–246.

De Magalhães J. P. Costa J. (2009). A database of vertebrate longevity records and their relation to other life-history traits. J. Evol. Biol. 22:1770–1774.

del Hoyo, J., Elliot, A., Sargatal, J., & Christie, D. A., eds (1992–2011). Handbook of the birds of the world. Vol. 1–16. Lynx Edicions, Barcelona.

DeSante D. F. Kaschube D. R. (2009). The monitoring avian productivity and survivorship (MAPS) program 2004, 2005, and 2006 report. Bird Pop. 9:86–169.

Dobson F. S. (2012). Lifestyles and phylogeny explain bird life histories. Proc. Nat. Acad. Sci. 109:10747–10748.

Dobson F. S. Oli M. K. (2007). Fast and slow life histories of mammals. Ecoscience 14:292–299.

DOF (2022). Dansk Ornitologisk Forening. Punkttællinger. https://www.dof.dk.

Dunning J. B. (2007). Handbook of Avian Body Masses (2nd ed). CRC Press, Boca Raton.

Eshel I. Motro U. (1981). Kin selection and strong evolutionary stability of mutual help. Theor. Pop. Biol. 19:420–433.

Fenchel T. (1974). Intrinsic rate of natural increase: The relationship with body size. Oecologia 14:317–326.

Fisher R. A. (1930). The genetical theory of natural selec-tion. Clarendon, Oxford.

Frost F., McCrea R., King R., Gimenez O., Zipkin E. (2023). Integrated population models: Achieving their potential. J. Stat. Theory Pract. 17:6.

Glazier D. S. (2005). Beyond the '3/4-power law': variation in the intra- and interspecific scaling of metabolic rate in animals. Biol. Rev. 80:611–662.

Gompertz B. (1832). On the Nature of the Function Expressive of the Law of Human Mortality, and on a New Mode of Determining the Value of Life Contingencies. Phil. Trans. R. Soc. Lond. 123:513–585.

Gregory R. D., Skorpilova J., Vorisek P., Butler S. (2019). An analysis of trends, uncertainty and species selection shows contrasting trends of widespread forest and farmland birds in Europe. Ecol. Indic. 103:676–687.

Griffiths D. (1977). Caloric variation in Crustacea and other animals. J. Anim. Ecol. 46:593–605.

Hairston N. G. J., Ellner S. P., Geber M. A., Yoshida T., Fox J. A. (2005). Rapid evolution and the convergence of ecological and evolutionary time. Ecol. Lett. 8:1114–1127.

Hardy I. C. W. Briffa M. (2013). Animal contests. Cambridge University Press, Cambridge.

Harvey P. H. Pagel M. D. (1991). The comparative method in evolutionary biology. Oxford University Press, Oxford.

Hendry A. P. (2017). Eco-evolutionary dynamics. Princeton University Press, Princeton.

Herberstein M. E., McLean D. J., Lowe1 E., Wolff J. O., Khan K., Smith K., Allen A. P., Bulbert M., Buzatto B. A., Eldridge M. D. B., Falster D., Winzer L. F., Griffith S. C., Madin J. S., Narendra A., Westoby M., Whiting M. J., Wright I. J., Carthey A. J. R. (2022). AnimalTraits – a curated animal trait database for body mass, metabolic rate and brain size. Sci. Data 9:265.

Hilborn R., Pikitch E. K., McAllister M. K. (1994). A Bayesian estimation and decision analysis for an age-structured model using biomass survey data. Fish. Res. 19:17–30.

Holder N. (1983). Developmental constraints and the evolution of vertebrate digit patterns. J. theor. Biol. 104:451–471.

Hudson L. N., Isaac N. J. B., Reuman D. C. (2013). The relationship between body mass and field metabolic rate among individual birds and mammals. J. Anim. Ecol. 82:1009–1020.

Jetz W., Sekercioglu C. H., Böhning-Gaese K. (2008). The worldwide variation in avian clutch size across species and space. PLOS Biol. 6:e303.

Johansson Ö., Ausilio G., Low M., Lkhagvajav P., Weck-worth B., Sharma K. (2021). The timing of breeding and independence for snow leopard females and their cubs. Mamm. Biol. 101:173–180.

Jones K. E., Bielby J., Cardillo M., Fritz S. A., O'Dell J.,

Orme C. D. L., Safi K., Sechrest W., Boakes E. H., Carbone C., Connolly C., Cutts M. J., Foster K. J., Grenyer R., Habib M., Plaster C. A., Price S. A., Rigby E. A., Rist J., Teacher A., Binninda-Emonds O. R. P., Gittleman J. L., Mace G. M., Purvia A. (2009). PanTHERIA: a species-level database of life history, ecology, and geography of extant and recently extinct mammals. Ecology 90:2648.

Kelt D. A. Van Vuren D. H. (2015). Home ranges of recent mammals. Ecology 96:1733.

Kendall B. E., Prendergast J., Bjørnstad O. N. (1998). The macroecology of population dynamics: taxonomic and biogeographic patterns in population cycles. Ecol. Lett. 1:160–164.

Kery M. Schaub M. (2011). Bayesian population analysis using WinBUGS. Academic Press, Amsterdam.

Kleiber M. (1932). Body and size and metabolism. Hilgardia 6:315–353.

Knape J. deValpine P. (2012). Are patterns of density dependence in the Global Population Dynamic Database driven by uncertainty about population abundance? Ecol. Lett. 15:17–23.

Knaus P., Schmid H., Strebel N., Sattler T. (2022). The State of Birds in Switzerland 2022 online. http://www.vogelwarte.ch.

Kolokotrones T., Savage V., Deeds E. J., Fontana W. (2010). Curvature in metabolic scaling. Nature 464:753–756.

Kozłowski J. Weiner J. (1997). Interspecific allometries are by-products of body size optimization. Am. Nat. 149:352–380.

Lanzarone E., Pasquali S., Gilioli G., Marchesini E. (2017). A Bayesian estimation approach for the mortality in a stage-structured demographic model. J. Math. Biol. 75:759–779.

Lee A. M., Bjørkvoll E. M., Hansen B. B., Albon S. D., Stien A., Sæther B. E., Engen S., Veiberg V., Loe L. E., Grøtan V. (2015). An integrated population model for a long-ived ungulate: more efficient data use with Bayesin methods. Oikos 124:806–816.

Lemaitre J. F., Ronget v., Tidiere M., Allaine D., Berger V., Cohas A., Colchero F., Conde D. A., Garratt M., Liker A., Marais G. A. B., Scheuerlein A., Szekely T., Gaillard J. M. (2020). Sex differences in adult lifespan and aging rates of mortality across wild mammals. Proc. Nat. Acad. Sci. 117:8546–8553.

Leung B., Hargreaves A. L., Greenberg D. A., McGill B., Dornelas M., Freeman R. (2020). Clustered versus catastrophic global vertebrate declines. Nature 588:267–273.

Linnaeus C. (1758). Systema naturae per regna tria naturae :secundum classes, ordines, genera, species, cum characteribus, differentiis, synonymis, locis. 10th ed. Laurentius Salvius, Stockholm.

Lloyd D. G. (1987). Selection of offspring size at independence and other size-versus-number strategies. Am. Nat. 129:800–817.

Lopez-Martin J. M., Casanovas R., Garcia-Petit J., Xifra J., Curia J., Canut J. (2013). Estatus y gestion del sarrio en el Pirineo catalan. In: Herrero J., Escuderi E., deLuco D. F., Garcia-Gonzalez R. (eds). El Sarrio Pirenaico Rupicapra p. pyrenaica: Biologia, Patologia Y Gestion: Publicaciones del Consejo de Proteccion de la Naturaleza de Aragon, pp 43–53.

LPI (2022). Living Planet Index database. www.livingplanetindex.org.

MacKay N. J. (2011). Mass scale and curvature in metabolic scaling. J. theor. Biol. 280:194–196.

Mahoney S. A. Jehl J. R. J. (1984). Body water content in marine birds. The Condor 86:208–209.

Makarieva A., Gorshkov V. G., Li B.-L. (2003). A note on metabolic rate dependence on body size in plants and animals. J. theor. Biol. 221:301–307.

Marco I., Rosell R., Cabezon O., Mentaberre G., Casas E., Velarde R., Lavin S. (2009). Border disease virus among Chamois, Spain. Emerg. Inf. Diseases 15:448–450.

Marquet P. A., Navarrete S. A., Castilla J. C. (1995). Body size, population density, and the energetic equivalence rule. J. Anim. Ecol. 64:325–332.

Maynard Smith J. (1971). The origin and maintenance of sex. In: Williams G. C. (ed). Group selection: Aldine Atherton, Chicago, pp 163–175.

Maynard Smith J. (1982). Evolution and the theory of games. Cambridge University Press, Cambridge.

Maynard Smith J. Price G. R. (1973). The logic of animal conflict. Nature 246:15–18.

McCarthy M. A., Citroen R., McCall S. C. (2008). Allometric scaling and Bayesian priors for annual survival of birds and mammals. Am. Nat. 172:216–222.

McKechnie A. E. Wolf B. O. (2004). The allometry of avian basal metabolic rate: Good predictions need good data. Physiolo Biochem Zool 77:502–521.

McKitrick M. C. (1993). Phylogenetic constraint in evolutionary theory: Has it any explanatory power? Ann. Rev. Ecol. Syst. 24:307–330.

McNab B. K. (2008). An analysis of the factors that influence the level and scaling of mammalian BMR. Comp. Bioch. Physiol. A 151:5–28.

MDD (2023). Mammal Diversity Database (Version 1.11) [Data set]. Zenodo.org DOI:10.5281/zenodo.7830771.

Millar J. S., Burkholder D. A. L., Lang T. L. (1986). Estimating age at independence in small mammals. Can. J. Zool. 64:910–913.

Murdoch W. W., Kendall B. E., Nisbet R. M., Briggs C. J., Mccauley E., Bolser R. (2002). Single-species models for many-species food webs. Nature 417:541–543.

Myhrvold N. P., Baldridge E. amd Chan B., Sivam D., Freeman D. L., Ernest S. K. M. (2015). An amniote life-history database to perform comparative analyses with

birds, mammals, and reltiles. Ecology 96:3109.

Nasrinpour H. R., Reimer A. A., Friesen M. R., McLeod R. D. (2017). Data preparation for West Nile Virus agent-based modelling: protocol for processing bird population estimates and incorporating ArcMap in AnyLogic. JMIR Res Protoc 6:e138.

Odum E. P., Marshall S. G., Marples T. G. (1965). The caloric content of migrating birds. Ecology 46:901–904.

Parker G. A. (1974). Assessment strategy and the evolution of fighting behaviour. J. theor. Biol. 47:223–243.

PECBMS (2022). Pan-European Common Bird Monitoring Scheme. https://pecbms.info.

Polansky L., De Valpine P., Lloyd-Smith J. O., Getz W. M. (2009). Likelihood ridges and multimodality in population growth rate models. Ecology 90:2313–2320.

Promilsow D. E. L. Harvey P. H. (1990). Living fast and dying young: a comparative analysis of life-history variation among mammals. J. Zool. 220:417—437.

Prothero J. W. (2015). The design of mammals. A scaling approach. Cambridge University Press, Cambridge.

Punt A. E. Butterworth D. S. (1999). On assessment of the Bering-Chukchi-Beaufort Seas stock of bowhead whales (*Balaena mysticetus*) using a Bayesian approach. J. Cetacean Res. Manage. 1:53–71.

Reeve H. K. Sherman P. W. (2001). Optimality and phylogeny: A critique of current thought. In: Orzack S. H. Sober E. (eds). Adaptation and optimality: Cambridge University Press, Cambridge, pp 64–113.

Richards F. J. (1959). A flexible growth function for empirical use. J. Exp. Bot. 10:290–300.

Ricklefs R. E. (2010). Embryo growth rates in birds and mammals. Funct. Ecol. 24:588–596.

Ricklefs R. E., Tsunekage T., Shea R. E. (2011). Annual adult survival in several new world passerine birds based on age ratios in museum collections. J. Ornithol. 152:481–495.

Roff D. A. (1992). The evolution of life histories. Theory and analysis. University of Chicago Press, New York.

Sæther B. E. Bakke O. (2000). Avian life history variation and contribution of demographic traits to the population gwowth rate. Ecology 81:642–653.

Salguero-Gomez R., Jones O. R., Archer C. R., Bein C., Buhr H., Farack C., Gottschalk F., Hartmann a., Henning A., Hoppe G., Romer G., Ruoff T., Sommer V., Wille J., Voigt J., Zeh S., Vieregg D., Buckle Y. M., Che-Castaldo J., Hodgson D., Scheuerlein A., Caswell H., Vaupe J. W. (2016). COMADRE: a global data base of animal demography. J. Anim. Ecol. 85:371–384.

Santini L., Isaac N. J. B., Ficetola G. F. (2018). TetraDEN-SITY: A database of population density estmates in terrestrial vertebrates. Global Ecol. Biog. 27:787–791.

SFT (2022). Svensk Fågeltaxering. http://www.fageltaxering.lu.se.

Sibly R. M., Baker D., Denham M. C., Hone J., Pagel M. (2005). On the regulation of populations of mammals,

birds, fish, and insects. Science 309:607–610.

Sibly R. M. Brown J. H. (2007). Effects of body size and lifestyle on evolution of mammal life histories. Proc. Nat. Acad. Sci. 104:17707–17712.

Sibly R. M., Witt C. C., Wright N. A., Venditti C., Jetz W., Brown J. H. (2012). Energetics, lifestyle, and reproduction in birds. Proc. Nat. Acad. Sci. 109:10937–10941.

Silva M., Brown J. H., Downing J. A. (1997). Differences in population density and energy use between birds and mammals: a macroecological perspective. J. Anim. Ecol. 66:327–340.

Sinervo B., Svensson E., Comendant T. (2000). Density cycles and an offspring quantity and quality game driven by natural selection. Nature 406:985–988.

Smith C. C. Fretwell S. D. (1974). The optimal balance between size and number of offspring. Am. Nat. 108:499–506.

Smith F. A., Brown J. H., Haskell J. P., Alroy J., Charnov E. L., Dayan T., Enquist B. J., Ernest S. K. M., Hadly E. A., Jablonski D., Jones K. E., Kaufman D. M., Lyons S. K., Marquet P., Maurer B. A., Niklas K., Porter W., Roy K., Tiffney B., Willig M. R. (2004). Similarity of mammalian body size across the taxonomic hierarchy and across space and time. Am. Nat. 163:672–691.

Stearns S. C. (1992). The evolution of life histories. Oxford University Press, Oxford.

Sulkava R. (2006). Ecology of the otter (Lutra lutra) in central Finland and methods for estimating the densities of populations. University of Joensuu, Biology PhD dissertation 0043.

Tamburello N., Cote I. M., Dulvy N. K. (2015). Energy and the scaling of animal space use. Amazoniana 186:196–211.

Taylor P. D. (1989). Evolutionary stability in one-parameter models under weak selection. Theor. Pop. Biol. 36:125–143.

Thompson J. N. (1998). Rapid evolution as an ecological process. Trends Ecol. Evol. 13:329–332.

Tobias J. A., Sheard C., Pigot A. L., et a. (2021). AVONET: morphological, ecological and geographical data for all birds. Ecol. Lett. 25:581–597.

Tucker M. A., Ord T. J., Rogers T. L. (2014). Evolutionary predictors of mammalian home range size: body mass, diet and the environment. Global Ecol. Biog. 23:1105–1114.

Turchin P. (1990). Rarity of density dependence or population regulation with lags? Nature 344:660–663.

Turchin P. Taylor A. D. (1992). Complex dynamics in ecological time series. Ecology 73:289–305.

Turcotte M. M., Reznick D. N., Hare J. D. (2011a). The impact of rapid evolution on population dynamics in the wild: experimental test of eco-evolutionary dynamics. Ecol. Lett. 14:1084–1092.

Turcotte M. M., Reznick D. N., Hare J. D. (2011b). Exper-

imental assessment of the impact of rapid evolution on population dynamics. Evol. Ecol. Res. 13:113–131.

Wade P. R. (2002). A Bayesian stock assessment of the Eastern pacific gray whale using abundance and harvest data from 1967–1996. J. Cetacean Res. Manage. 4:85–98.

Weisbecker V., Ashwell K., Fisher D. (2013). An improved body mass dataset for the study of Marsupial brain size evolution. Brain Behav. Evol. 13:81–82.

West G. B., Brown J. H., Enquist B. J. (1997). A general model for the origin of allometric scaling laws in biology. Science 276:122–126.

West G. B., Brown J. H., Enquist B. J. (1999). The fourth dimension of life: fractal geometry and allometric scaling of organisms. Science 284:1677–1679.

Williams G. C. (1975). Sex and evolution. Princeton University Press, Princeton.

Wilson, D. E. & Mittermeier, R. A., eds (2009–2014). Handbook of the mammals of the world. Vol. 1–4. Lynx Edicions, Barcelona.

Witteman G. J., Redfearn A., Pimm S. L. (1990). The extent of complex population changes in nature. Evol. Ecol. 4:173–183.

Witting L. (1995). The body mass allometries as evolutionarily determined by the foraging of mobile organisms. J. theor. Biol. 177:129–137, https://doi.org/10.1006/jtbi.1995.0231.

Witting L. (1997). A general theory of evolution. By means of selection by density dependent competitive interactions. Peregrine Publisher, Århus, 330 pp, URL https://mrLife.org.

Witting L. (2000a). Interference competition set limits to the fundamental theorem of natural selection. Acta Biotheor. 48:107–120, https://doi.org/10.1023/A:1002788313345.

Witting L. (2000b). Population cycles caused by selection by density dependent competitive interactions. Bull. Math. Biol. 62:1109–1136, https://doi.org/10.1006/bulm.2000.0200.

Witting L. (2002). From asexual to eusocial reproduction by multilevel selection by density dependent competitive interactions. Theor. Pop. Biol. 61:171–195, https://doi.org/10.1006/tpbi.2001.1561.

Witting L. (2007). Behavioural interactions selecting for symmetry and asymmetry in sexual reproductive systems of eusocial species. Bull. Math. Biol. 69:1167–1198, https://doi.org/10.1007/s11538–006–9112–x.

Witting L. (2008). Inevitable evolution: back to *The Origin* and beyond the 20th Century paradigm of contingent evolution by historical natural selection. Biol. Rev. 83:259–294, https://doi.org/10.1111/j.1469–185X.2008.00043.x.

Witting L. (2013). Selection-delayed population dynamics in baleen whales and beyond. Pop. Ecol. 55:377–401, https://dx.doi.org/10.1007/s10144–013–0370–9.

Witting L. (2017a). The natural selection of metabolism and mass selects allometric transitions from prokaryotes to mammals. Theor. Pop. Biol. 117:23–42, https://dx.doi.org/10.1016/j.tpb.2017.08.005.

Witting L. (2017b). The natural selection of metabolism and mass selects lifeforms from viruses to multicellular animals. Ecol. Evol. 7:9098–9118, https://dx.doi.org/10.1002/ece3.3432.

Witting L. (2018). The natural selection of metabolism explains curvature in allometric scaling. Oikos 127:991–1000, https://dx.doi.org/10.1111/oik.05041.

Witting L. (2020). The natural selection of metabolism explains curvature in fossil body mass evolution. Evol. Biol. 47:56–75, https://dx.doi.org/10.1007/s11692–020–09493–y.

Witting L. (2023a). On the natural selection of body mass allometries. Acta Oecol. 118:103889, https//dx.doi.org/10.1016/j.actao.2023.103889.

Witting L. (2023b). Population dynamic population delineation in North American birds. Preprint at bioRxiv https://dx.doi.org/10.1101/2023.08.29.555290.

Witting L. (2023c). On natural selection regulation in the population dynamics of birds and mammals. Preprint at bioRxiv https://dx.doi.org/10.1101/2021.11.27.470201.

Wolda H. Dennis B. (1993). Density-dependence tests, are they. Oecologia 95:581–591.

Ziehm M., Ivanov D. K., A. B., Partridge L., Thornton J. M. (2015). SurvCurv database and online survival analysis platform update. Bioinformatics 31:3878–3880.

Appendix

A   Demography

I estimate the demography of stable populations with a per-generation growth rate of unity

$$\lambda = l_m R/2 = 1 \qquad (10)$$

with l_m being the probability that a newborn survives to the age of maturity, and R the expected lifetime reproduction of females that survive to t_m, assuming an even sex ratio.

Data on age-structured reproduction and survival are becoming increasingly available (e.g., Lemaitre et al. 2020), yet structured estimates are unavailable most often. Hence, I use an average annual birth rate (m) across all mature females, and a constant adult survival (p_{ad}) that reflects the estimates of the literature. These are usually some average across an unspecified range of age classes around the age-structured peak in reproduction and survival, before the unset of senescence.

Expected lifetime reproduction

$$R = t_r m \qquad (11)$$

is given as the product between the annual birth rate (m) and the expected reproductive period (t_r). With $l_a = \prod_{x=0}^{a-1} p_x$ being the survival curve over age (a), the expected reproductive period is

$$
\begin{aligned}
t_r &= \sum_{a=t_m}^{t_l} l_a/l_m \qquad (12) \\
&= 1 + p_{t_m} + p_{t_m} p_{t_{m+1}} + \ldots + p_{t_m} p_{t_{m+1}} \cdots p_{t_l} \\
&= 1 + \sum_{i=t_m}^{t_l} \prod_{a=t_m}^{i} p_a = \sum_{i=0}^{\infty} p^i = \frac{1}{1-p}
\end{aligned}
$$

where p (no subscript) is annual adult ($a \geq t_m$) survival in the age-structured population dynamic model of Appendix C.

With p_{ad} being survival among some of the best surviving age classes, we have $p < p_{ad}$ and $t_r < 1/(1-p_{ad})$. And given $\tilde{p}_0 = p_{a=0}/p_{ad} < 1$, we have $l_m = \tilde{p}_0 p_{ad}^{t_m}$ given that $p_a = p_{ad}$ for $a > 0$. Then, as $l_m = 2/mt_r$ from eqns 10 and 11, we have $t_r = 2/m\tilde{p}_0 p_{ad}^{t_m}$. With a median $\tilde{p}_0$ estimate of 0.52 across more than 500 birds (Beauchamp 2023), I use

$$t_r = \min\left[\frac{4}{mp_{ad}^{t_m}}, \frac{1}{1-p_{ad}}\right] \qquad (13)$$

as an estimate of the expected reproductive period.

Following Charlesworth (1980), a useful measure of generation time is mean reproductive age

$$t_g = \frac{\sum_{a=t_m}^{t_l} a\, m_a\, l_a}{\sum_{a=t_m}^{t_l} m_a\, l_a} \qquad (14)$$

Given constant yearly reproduction (m), generation time reduces to

$$
\begin{aligned}
t_g &= \frac{m\, l_m \sum_{a=t_m}^{t_l} a\, l_a/l_m}{m\, l_m \sum_{a=t_m}^{t_l} l_a/l_m} \qquad (15) \\
&= t_m + \frac{\sum_{a=t_m}^{t_l} (a-t_m) l_a/l_m}{\sum_{a=t_m}^{t_l} l_a/l_m} \\
&= t_m + \frac{\sum_{i=0}^{\infty} i p^i}{\sum_{i=0}^{\infty} p^i} \\
&= t_m + \frac{p}{1-p} = t_m + t_r - 1
\end{aligned}
$$

as $p/(1-p) = t_r - 1$ given $p = (t_r - 1)/t_r$ from eqn 12 where $0 < p < 1$ and $t_r > 1$. Before calculating t_g, time is scaled to timesteps (Δt) that ensure $t_r/\Delta 1 > 1$.

B   Estimation sequence

After the removal of outliers (outlier SI), I filtered (filter SI) data on individual growth, lifespan, and survival, and calculated mortality ($q_{ad} = 1 - p_{ad}$) from survival (p_{ad}) for all accepted survival data. I calculated the $\beta/\underline{\beta}$ ratio of field (β) over basal ($\underline{\beta}$) metabolism for all species data on both and used a $\beta/\underline{\beta}$ invariance estimator to obtain data-like values of both β and $\underline{\beta}$ for all species with a data estimate of at least one of the two rates. Missing values were then estimated by interspecific extrapolations for m_b, m_f, t_p, t_j, t_m, t_l, p_{ad}, q_{ad}, $\tilde{w}_0$, $\tilde{w}_j$, z, β, $\underline{\beta}$, h, and N.

The missing value estimates for p_{ad} and q_{ad} were adjusted to identical mirror values to avoid unrealistic estimates where $p_{ad} > 1 \wedge q_{ad} < 0$ or $p_{ad} < 0 \wedge q_{ad} > 1$. With $\bar{p_{ad}}$ being the average survival rate for the two missing parameter estimates of p_{ad} and q_{ad}, the adjustment was done by setting $q_{ad} = 1 - p_{ad}$ for $\bar{p_{ad}} \leq 0.25$, by setting $p_{ad} = 1 - q_{ad}$ for $\bar{p_{ad}} \geq 0.75$, and setting $p_{ad} = \bar{p_{ad}}$ and $q_{ad} = 1 - \bar{p_{ad}}$ for $0.25 < \bar{p_{ad}} < 0.75$.

I then filtered all survival estimates, and calculated $m = m_b m_f$ and w_f from eqn 2. t_r was calculated by eqn 13 and filtered for lower outlier values (see filter SI) before all lifespan estimates were filtered. I then calculated t_g by eqn 14, $R = t_r m$, and $l_m = 2/t_r m$ by eqn 10. $\bar{w}_j$ was estimated by eqn 6, net energy as $\epsilon = w_e \acute{\beta} R/t_r$, gross energy as $\epsilon_g = w\beta + \epsilon/2$ (and filtered by the gross energy filter), resource handling as

$\alpha = \epsilon/\beta$, home range overlap as $h_o = hN$, encounter rate as $v = \beta w^{1/2d}/h^{1/d}$, and the level of interference as $I = h_o v$ followed by a rescaling to set $\iota = \ln I$ equal to unity at the median across all birds.

C   Population dynamics

The age-structured population dynamic model is parameterised from annual reproduction (m), the age of reproductive maturity (t_m), and the reproductive period (t_r), in years. These estimates are converted to $m^* = m\Delta t$, $a_m = t_m/\Delta t$, and $a_r = t_r/\Delta t$ with the number of iteration timesteps per year ($1/\Delta t$) being adjusted to ensure $\min(a_m, a_r) > 1$. The $p = (a_r - 1)/a_r$ survival from eqn 12 apply to all age-classes except age-class zero, where survival is $p_0 = l_m/p^{a_m - 1}$ given $l_m = 2/a_r m^*$.

With $x \gg a_m$ being the maximum lumped age-class, the number $n_{a,t}$ of individuals of age $0 < a < x$ at timestep t is

$$n_{a,t} = p_{a-1} n_{a-1,t-1} \qquad (16)$$

and the number in age-class x

$$n_{x,t} = p_x n_{x,t-1} + p_{x-1} n_{x-1,t-1} \qquad (17)$$

with $p_a = p_0$ for $a = 0$ and $p_a = p$ for $a \geq 1$. Let the number of individuals in each age-class relate to time just after each timestep transition, with offspring at t being produced by the $t - 1$ individuals that survive to the $t - 1 \to t$ transition, with the density-dependent ecology being approximated by the average 1+ abundance of the two timesteps:

$$\hat{n}_t = 0.5 \sum_{a \geq 1} n_{a,t} + n_{a,t-1} \qquad (18)$$

The number of offspring in age-class zero is then

$$n_{0,t} = 0.5 \, m^* \left(\frac{\hat{n}^*}{\hat{n}_t}\right)^\gamma \sum_{a \geq a_m} \tilde{m}_{a,t} \, n_{a,t} \qquad (19)$$

where γ is the strength of density regulation, and $\tilde{m}_{a,t} = 1/q_{a,t}$, with $q_{a,t}$ being the average competitive quality of cohort a at t. At the population dynamic equilibrium $q_a^* = 1$ for all ages. More generally $q_{a,t} = q_{a-1,t-1}$ and

$$q_{x,t} = \frac{q_{x,t-1} p_x n_{x,t-1} + q_{x-1,t-1} p_{x-1} n_{x-1,t-1}}{n_{x,t}} \qquad (20)$$

assuming that there is no change in the quality of a cohort over time. The quality of offspring

$$q_{0,t} = \frac{\sum_{a \geq a_m} q_{a,t} \, n_{a,t}}{\sum_{a \geq a_m} n_{a,t}} \left(\frac{\hat{n}_t}{\hat{n}^*}\right)^{\gamma_\iota} \qquad (21)$$

is the average quality of the mature component multiplied by the density-dependent selection, with γ_ι being the selection response.

For the initial conditions of an iteration I use the same quality across all individuals, and an initial abundance with a stable age-structure

$$c_a = l_a / \sum_{a \geq 0} l_a \qquad (22)$$

where $l_0 = 1$, $l_a = p_0 \, p^{a-1}$ for $1 \leq a < x$, and $l_x = p_0 \, p^{x-1}/(1 - p)$.

D   Supplementary Information

Supplementary Information to this article can be found online at https://doi.org/10.1016/j.ecoinf.2024.102492.